

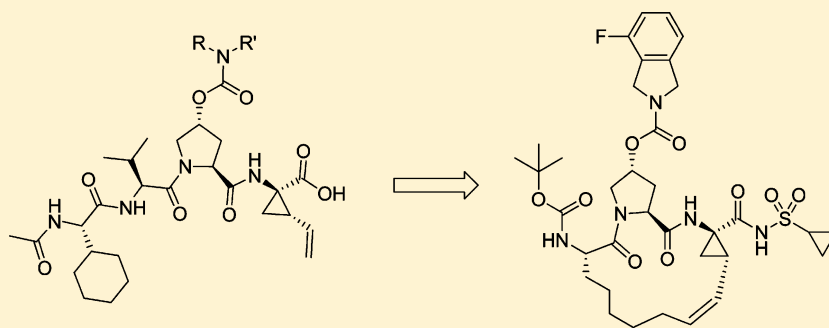
Discovery of Danoprevir (ITMN-191/R7227), a Highly Selective and Potent Inhibitor of Hepatitis C Virus (HCV) NS3/4A Protease

Yutong Jiang,^{*,†} Steven W. Andrews,[†] Kevin R. Condroski,[†] Brad Buckman,[‡] Vlad Serebryany,[‡] Steve Wenglowksy,[†] April L. Kennedy,[†] Machender R. Madduru,[†] Bin Wang,[†] Michael Lyon,[†] George A. Doherty,[†] Benjamin T. Woodard,^{†,§} Christine Lemieux,[†] Mary Geck Do,[†] Hailong Zhang,[†] Joshua Ballard,[†] Guy Vigers,[†] Barbra J. Brandhuber,[†] Peter Stengel,[†] John A. Josey,[†] Leonid Beigelman,[‡] Lawrence Blatt,[‡] and Scott D. Seiwert[‡]

[†]Array BioPharma, 3200 Walnut Street, Boulder, Colorado 80301, United States

[‡]InterMune Inc., 3280 Bayshore Boulevard, Brisbane, California 94005, United States

S Supporting Information



Danoprevir (49)

ABSTRACT: HCV serine protease NS3 represents an attractive drug target because it is not only essential for viral replication but also implicated in the viral evasion of the host immune response pathway through direct cleavage of key proteins in the human innate immune system. Through structure-based drug design and optimization, macrocyclic peptidomimetic molecules bearing both a lipophilic P2 isoindoline carbamate and a P1/P1' acylsulfonamide/acylsulfamide carboxyic acid bioisostere were prepared that possessed subnanomolar potency against the NS3 protease in a subgenomic replicon-based cellular assay (Huh-7). Danoprevir (compound 49) was selected as the clinical development candidate for its favorable potency profile across multiple HCV genotypes and key mutant strains and for its good in vitro ADME profiles and in vivo target tissue (liver) exposures across multiple animal species. X-ray crystallographic studies elucidated several key features in the binding of danoprevir to HCV NS3 protease and proved invaluable to our iterative structure-based design strategy.

INTRODUCTION

Hepatitis C virus (HCV) infection afflicts approximately 150 million people worldwide, with 3–4 million new infections every year.^{1a} HCV infections may present few initial symptoms but over time can lead to liver fibrosis, cirrhosis, and hepatocellular carcinoma, making HCV the leading cause of liver transplantation in the United States and more than 350000 annual deaths globally.¹ Prior to the arrival of direct acting antivirals (DAAs), the standard of care (SoC) for chronic HCV infection was pegylated interferon alpha (PEG IFN- α) in combination with ribavirin (RBV), which provided sustained virologic response (SVR) in about 50% of treated patients and was associated with significant side effects.² In the past decade, major drug discovery endeavors have focused on combating HCV with DAAs,³ which target essential enzymes encoded by hepatitis C virus, such as nonstructural proteins NS3/4A, NSSA,^{4a} and NSSB.^{4b}

The NS3/4A is a chymotrypsin-like serine protease that plays an essential role in the HCV viral replication process. Small molecule DAAs inhibiting the NS3 proteolytic activity can achieve rapid viral load drop in patients, as was first demonstrated with inhibitor ciluprevir by Boehringer Ingelheim in 2002.^{5a,b} In addition to its crucial role of processing viral polypeptide, the NS3/4A protease has also been shown to dampen cellular sensing of viral components, thus reducing endogenous type 1 interferon production.⁶ Therefore, an NS3 protease inhibitor would potentially suppress HCV replication by simultaneously disrupting two processes critical to the survival of the virus.

Special Issue: HCV Therapies

Received: January 31, 2013

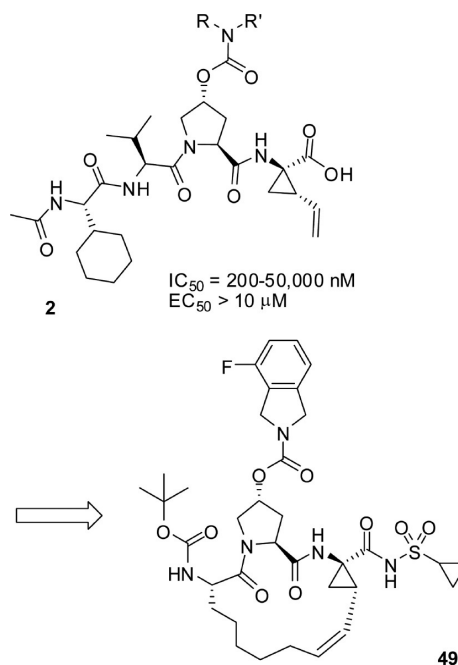
In 2011, two first-generation DAAs, HCV NS3 protease inhibitors telaprevir⁷ and boceprevir,⁸ were approved by the FDA. The new treatment regimens significantly improved overall SVR from the previous 50% range to around 70%, but these inhibitors must still be administered in combination with the old SoC (PEG IFN- α /RBV) in order to prevent the rapid emergence of resistance.^{7c,8c} The side effects brought on by these triple combination therapies can compromise their clinical utility due to treatment discontinuation. In addition, to many parts of the world, interferon is still prohibitively expensive and can deter chronic HCV patients from seeking treatments in the first place. Therefore, a high unmet medical need exists to develop second-generation DAAs with milder adverse effects, high barriers to resistance, and action through multiple inhibition mechanisms, eventually leading to a future SoC that is IFN-sparing. Some of the second-generation NS3 protease inhibitors currently under advanced clinical investigations include: simeprevir (TMC435350),^{5c} faldaprevir (BI201335),^{5d} vaniprevir (MK-7009),^{5e} and MK-5172.^{5f}

Our drug discovery campaign aims at maximizing inhibitor potency across HCV genotypes and clinically relevant drug-resistant strains (i.e., A156T and D168A), minimizing off-target activities and optimizing compound preferential tissue distribution to the liver, the primary HCV replication site. Herein we report the structure-based design, SAR investigation, and the ensuing DMPK optimization that lead to the discovery of a novel HCV NS3/4A protease inhibitor danoprevir (ITMN-191/R7227). Danoprevir is a macrocyclic noncovalent reversible NS3 inhibitor with a slow-off rate.^{9f} It displays unique preclinical characteristics and elicits potent antiviral activity in the clinic.^{9,10} Currently, danoprevir is in phase II clinical development both in combination with PEG IFN- α /RBV and with NSSB inhibitor mericitabine.

■ STRUCTURE-BASED DESIGN AND INITIAL LEADS

At the outset of this work, the available X-ray crystallographic structures of the NS3 protease domain revealed a relatively shallow and highly solvent-exposed active site. This binding pocket presented a challenging task in designing selective and potent small molecule inhibitors against the HCV NS3 protease. To pursue our novel class of NS3 inhibitors, a virtual chemical library was first designed and evaluated in docking studies using GOLD.^{14a} This virtual library consisted of tetrapeptides that possessed a P1/P1' carboxylic acid headgroup and probed diverse P2 substituents that occupy the lipophilic S2 protein surface region (1, Scheme 1). Selection of the most promising chemical targets was based upon a consensus scoring technique that was subsequently applied to the GOLD docking results.^{14b} This smaller set was then synthesized as a focused library of P2 carbamates (2). Gratifyingly, the inhibition results from the NS3 enzymatic assay demonstrated that the virtual screening picks clustered around the most potent hits, supporting the validity of our proposed inhibitor binding mode. After several iterations of P2 optimization, we identified a P2 tetrahydroisoquinoline (THIQ) carbamate as a promising lead (3).

Although compound 3 was significantly potent in the NS3 enzyme functional assay, it showed no cellular potency in a replicon-based assay at its top titration level (10 μ M). This was attributed to the compound's poor cell permeability as a result of high polar surface area (solvent accessible PSA = 187 Å²), three hydrogen-bond donors, and a charged carboxylic acid. To solve this problem, we opted to first transform the small peptide to a macrolide so that the molecule's highly exposed polar surface



IC₅₀ = 0.2–0.4 nM (1a, 1b, 4, 5 & 6), 1.6 nM (2b), 3.5 nM (3a)
 EC₅₀ = 1.6 nM (1b), 20 nM (2 & 3)
 MT4-MTT CC₅₀ = 54 μ M
 CYP 1A2, 2C19, 2C9, 2D6 > 25 μ M; 3A4 = 12 μ M
 Time-dependent CYP3A4 inhibition/induction: Negative
 hERG %block @ 10 μ M: Negative
 Selectivity: IC₅₀ > 10 μ M in panel of 53 proteases
 Oral bioavailability (liver): 15 % (rat); 78 % (monkey)
 Liver/plasma ratio: ~10 (rat); ~30 (dog); ~100 (monkey)

area is partially shielded and the labile amide bonds are rigidified, both of which aimed at improving cell permeability and metabolic stability.¹¹ Aided by computational modeling, we linked the P1 and P3 side chains of 3 to form a 15-membered macrocyclic acid 4. This modification indeed increased the compound's replicon potency to approximately 2 μ M, with enzymatic potency equivalent to its tetrapeptide predecessor. To further improve cell permeability, we tested the replacement of the carboxylic acid P1 headgroup with an acid bioisostere acylsulfonamide, reasoning that while still maintaining an acidic group, acylsulfonamide could better distribute the anionic charge over additional atoms, hence increasing cell permeability.¹² In addition, our docking studies also suggested that an alkyl sulfonamide could simultaneously fill the S1' pocket and form additional hydrogen bonds in the oxyanion hole, further improving the inhibitor's binding affinity. The resulting cyclopropyl sulfonamide 5 improved both enzymatic and cellular potency by more than 2 orders of magnitude. This dramatic improvement demonstrated that the acylsulfonamide indeed provided superior cell permeability as well as increase in binding affinity. Although these exciting results validated our drug-design approach, the magnitude of improvement was unexpected.

As shown in Figure 1, the X-ray cocrystal structure of a close analogue of 5 [in which the P3 *t*-butyl carbamate was replaced by a cyclopentyl carbamate (6, IC₅₀ = 1 nM, EC₅₀ = 6 nM)] was obtained bound in the NS3 protease domain active site. This result provided experimental support for our docking hypothesis and initial SAR observations: (1) the peptide backbone of the molecule forms tight β -sheet-like interactions with the protein, (2) the acylsulfonamide is well positioned for multiple hydrogen-

Scheme 1. Structure-Based Library Design to Lead 5 through Depeptidization and P2, P1' Modifications

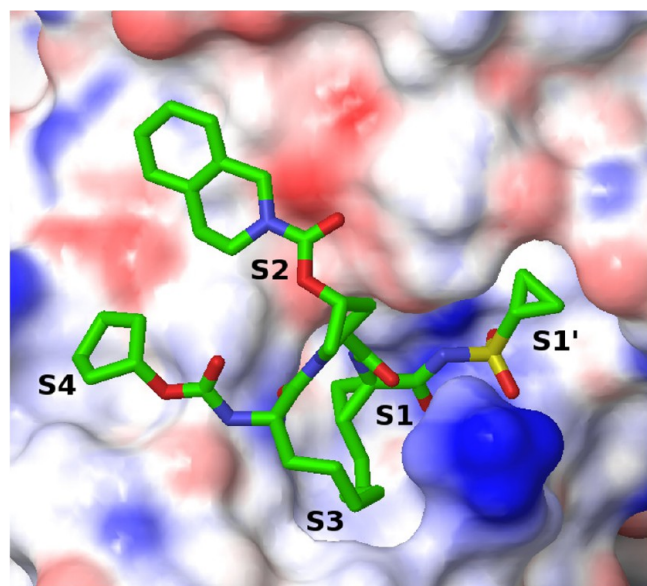
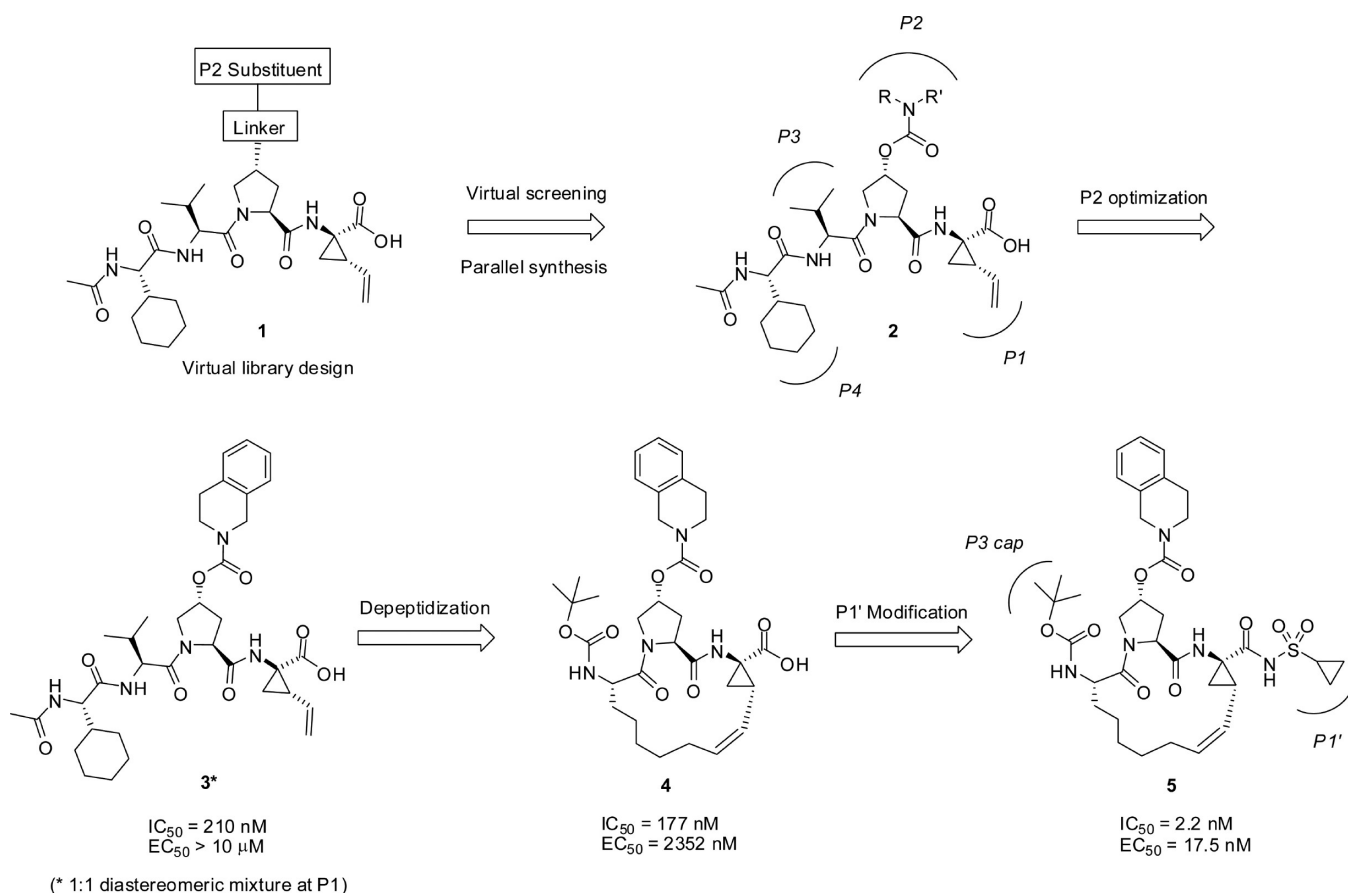


Figure 1. X-ray crystal structure of inhibitor **6** bound to HCV NS3 protease (PDB 4KTC).

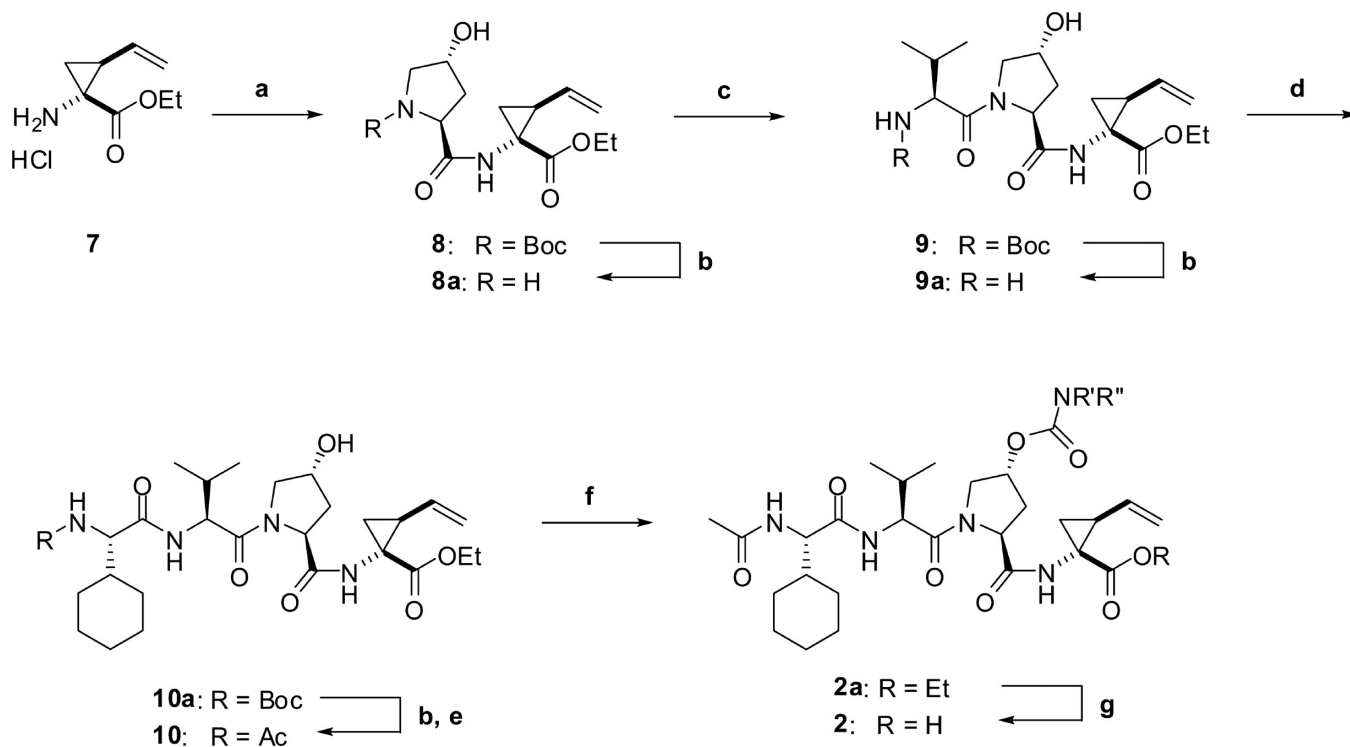
bond interactions with protein active site residues G137, S138 and S139, (3) the cyclopropyl P1' group binds effectively in the S1' pocket, (4) neither the P2 carbamate linker nor the THIQ group appears to form any specific interactions with the protein. However, the largely flat and lipophilic THIQ group likely achieves binding affinity by conforming closely atop the flat, lipophilic "peninsula" on the S2 region of the protein surface,

which is primarily composed of hydrophilic surface residues. This crystal structure provided the starting point for the structure-based design of our HCV protease inhibitors with improved potency and pharmacokinetic profiles.

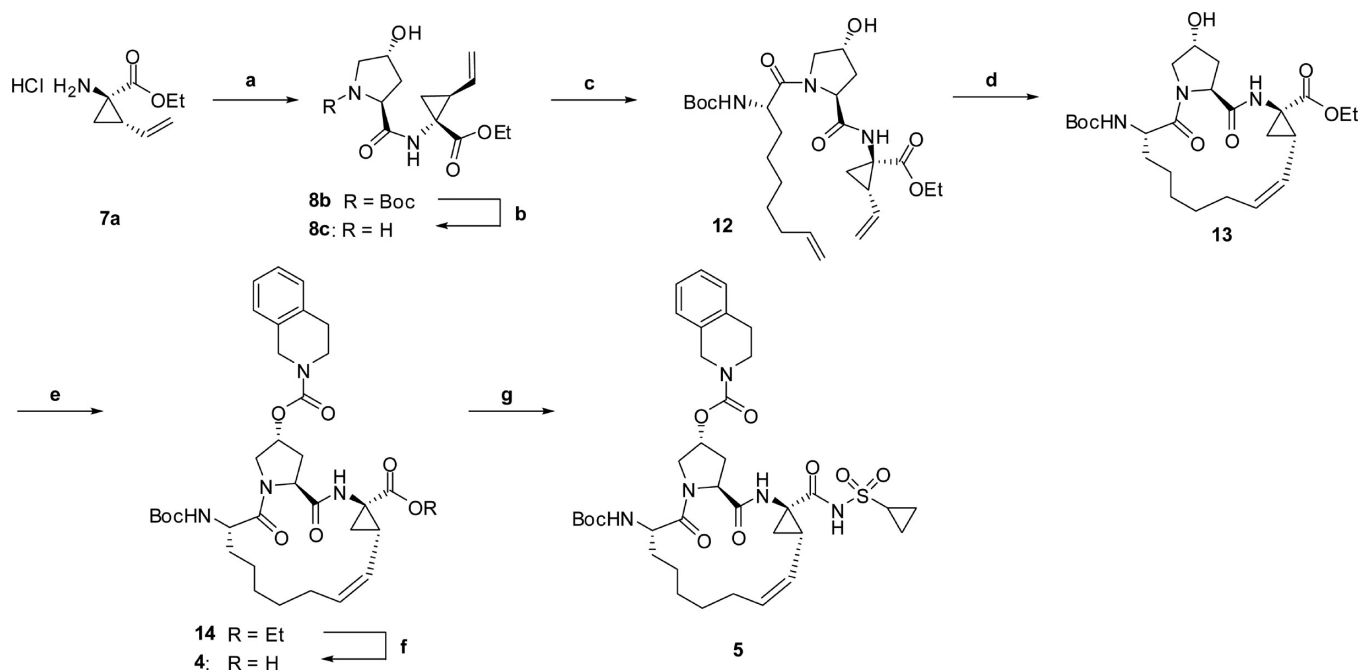
CHEMISTRY

The synthesis of the tetrapeptide P2-carbamate chemical library is shown in Scheme 2. Initially, racemic P1 vinyl cyclopropyl amino acid (**7**) was used, which was later replaced by the active enantiomer (**7a**, Scheme 3) at the lead optimization stage. Through HATU-facilitated peptide coupling steps a, c, and d, compound **10** was readily obtained as a common intermediate. After surveying various carbamate-forming reactions, we selected the CDI method (step e) for its ready access to our desired amine inputs and clean reaction profile suitable for parallel syntheses. As the last step, the final compounds **2** were obtained through mild hydrolysis without any observed deterioration of enantiomeric purity.

The route used to prepare the macrocyclic P1/P1' acylsulfonamide **5** is shown in Scheme 3. The enantiomerically enriched (>99% ee) P1 vinyl cyclopropyl amino acid (**7a**) was prepared from an enzymatic resolution of the racemic mixture **7**.¹⁶ The P3 long chain amino acid (**11**) was initially obtained from a commercial source and later prepared based on literature precedent.¹⁶ Through HATU-facilitated peptide coupling steps, intermediate **12** was prepared in good yield without the need to protect the P2 hydroxyl group. Using the same CDI-mediated coupling method as in Scheme 2, the P2 carbamate motif was then attached to the macrocyclic hydroxyproline intermediate **13**. This method was amenable to rapid analogue synthesis. The

Scheme 2^a

^aReaction conditions: (a) (2*S*,4*R*)-1-(*tert*-butoxycarbonyl)-4-hydroxypyrrolidine-2-carboxylic acid, HATU, DIEA, DMF, 81%; (b) HCl, dioxane, 99%; (c) (*S*)-2-(*tert*-butoxycarbonylamino)-3-methylbutanoic acid, HATU, DIEA, DMF; (d) (*S*)-2-(*tert*-butoxycarbonylamino)-2-cyclohexylacetic acid, HATU, DIEA, DMF, 59%; (e) AcOH, HATU, DIEA, DMF, 60%; (f) (i) CDI, DCM, 25 °C, (ii) R'R''NH, DCM, 25 °C; (g) LiOH-H₂O, THF/MeOH/H₂O 2:2:1.

Scheme 3^a

^aReaction conditions: (a) (2*S*,4*R*)-1-(*tert*-butoxycarbonyl)-4-hydroxypyrrolidine-2-carboxylic acid, HATU, DIEA, DMF, 80%; (b) HCl, dioxane, 99%; (c) (*S*)-2-(*tert*-butoxycarbonylamino)non-8-enoic acid (11), HATU, DIEA, DMF, 87%; (d) 5 mol % RCM catalyst, DCE, 50 °C, 52%; (e) (i) CDI, DCM, 25 °C, (ii) 1,2,3,4-tetrahydroisoquinoline, DCM, 25 °C, 90%; (f) LiOH-H₂O, THF/MeOH/H₂O 2:2:1, 87%; (g) (i) CDI, DCE, 50 °C, (ii) cyclopropanesulfonamide (15), DBU, 50 °C, 94%.

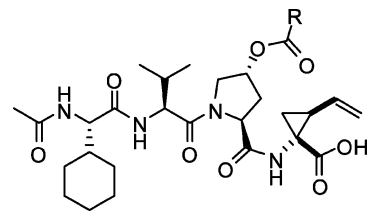
ring-closing-metathesis (RCM) step from **12** to **13** was accomplished in the presence of a variety of catalyst systems with similarly good yields and purity.¹⁶ The polymeric impurities generated from the RCM step were easily removed via a silica gel plug, followed by crystallization of **13** directly from the filtrate. In the final steps, carboxylic acid **4** was first activated with CDI and then coupled to cyclopropanesulfonamide in the presence of DBU to readily yield the final product **5**. As before, no deterioration of enantiomeric purity was observed throughout this synthetic sequence.

DISCUSSION

The P2 carbamate tetrapeptide inhibitors prepared from the focused library (**2**, Scheme 1) were tested for their inhibitory effect on the NS3 protease activity in cleaving a quenched-fluorogenic substrate, RET S1 (AnaSpec Inc., Ac-DED-(EDANS)EEAbu Ψ[COO]ASK(DABCYL)), in a continuous fluorescence resonance energy transfer (FRET) assay. IC₅₀ values were determined using a four-parameter curve fit equation, and potent compounds were then evaluated in a subgenomic replicon-based ELISA cellular assay that quantifies the HCV viral replication level using a selectable marker protein, Neomycin phosphotransferase II (NPTII). EC₅₀ values, the compound concentrations required to achieve 50% inhibition of the HCV viral RNA replication in Huh-7 hepatoma cells as compared to a DMSO-treated control signal, were calculated using a four-parameter curve fit equation as well. This ELISA quantification assay showed strong correlation to Taqman RNA analysis method. All biochemical and cellular data reported here are an average of at least three individual measurements ($n \geq 3$). In all cases, individual measurements were within 3-fold for each compound. As mentioned earlier, none of the inhibitors from library **2** showed detectable inhibitory effect in this cellular assay at up to 10 μM concentration. Subsequent macrocyclic analogues with much enhanced cell potency (e.g., **5**) were further tested for inhibitory activity in a panel of protease functional assays (e.g., cathepsin B, chymotrypsin, thrombin, and leukocyte elastase) to gauge the selectivity profile of this lead series. Representative inhibitors were also evaluated for their inhibitory effect on hERG channel activity at 1, 5, and 10 μM levels. In vivo plasma and liver drug exposures were examined both intravenously and orally in rats for selected inhibitors that met our replicon potency and in vitro hepatic stability criteria. Orally dosed compounds with target tissue (liver) exposures above predicted efficacious levels would then be advanced into higher species including monkeys and dogs for additional PK studies on liver and plasma drug exposures.

P2 Carbamate Initial Tetrapeptide Leads. A chemical library of about 70 tetrapeptides bearing carbamates attached to the P2 hydroxyproline was synthesized utilizing a diverse set of primary and secondary amine inputs (**2**, Scheme 1). Key results from this series are summarized in Table 1. A clear trend in the SAR emerged by which an appropriately placed lipophilic group, preferably a fused or pendent aromatic, provided significant increase in NS3 enzyme inhibition. For example, the simple phenyl and benzyl carbamates (**16** and **18**) were micromolar inhibitors, while aryl ring substituents failed to provide any significant potency improvement (data not shown). However, the naphthyl analogues (**17** and **19**) provided a 3- to 4-fold increase in potency and the first submicromolar inhibitors in this series. The unexpected improvement in potency by incorporating an appropriately positioned aromatic group extended to heterocyclic templates as well. The morpholine carbamate **20**

Table 1. Inhibitory Activity against HCV NS3 for P2 Carbamate Tetrapeptide Lead Series



Cmpd	R	IC ₅₀ (nM)
16		3,440
17		835
18		2,755
19		818
20		47,103
21		4,769
22		5,500
23		4,286
3		210
24		14,877
25		735
26		200
27		186

was essentially inactive, while the 2- and 3-phenylmorpholine carbamates **21** and **22** demonstrated an order of magnitude improvement in potency. Piperidine carbamate **23** was a weakly potent inhibitor at 4.3 μM, whereas tetrahydroisoquinoline carbamate **3** was 20-fold more potent at 210 nM. Likewise,

pyrrolidine carbamate **24** was nearly inactive; however, 3-phenyl pyrrolidine, indoline, and isoindoline carbamates (**25**, **26**, and **27**) demonstrated up to an 80-fold increase in potency at 735, 200, and 186 nM, respectively. The surprising SAR from this series clearly suggests that (1) lipophilic interactions in the S2 pocket provide significant enhancements in potency, and (2) fused bicyclic amines were the optimal P2 groups for accessing this space through a carbamate linker. From this library, compound **3** was selected as a tool molecule for further enhancing cellular potency.

P2 Carbamate Macrocylic Leads. The lack of cell potency in the tetrapeptide series was ascribed to poor cell permeability. Two depeptidization strategies were therefore implemented: truncation of the P4 amino acid and macrocyclization of the resulting tripeptide. Both strategies aimed at reducing the solvent exposed polar surface areas of the tetrapeptide lead, while macrocyclization would also rigidify the peptide backbone and protect the amide bonds from proteolytic cleavage. Truncation and macrocyclization of inhibitor **3** led to 15-membered macrocyclic tripeptide mimetic **4**. This compound retained the same level of enzymatic potency (IC_{50} = 177 nM) as its tetrapeptide predecessor **3** (IC_{50} = 210 nM), indicating that the newly formed 15-membered macrocyclic ring system did not disrupt any key inhibitor–enzyme binding site interactions. Thus, the SAR that had been established for the tetrapeptide lead series should be analogous to the new macrocyclic series. More importantly, compound **4** marked the program's first NS3 inhibitor with antiviral activity inside human cells (replicon EC_{50} = 2352 nM) and validated the improvement in cell permeability by the above depeptidization approaches.

To further improve potency and reduce the EC_{50}/IC_{50} ratio of inhibitor **4** (~ 10), the P1/P1' carboxylic acid group was replaced with an acylsulfonamide as a carboxylic acid bioisostere. It was postulated that the greater delocalization of negative charge around the acylsulfonamide versus the carboxylic acid would lead to increased cell permeability. Furthermore, molecular modeling suggested that additional binding interactions could be gained between the extended P1' group and the S1' binding pocket of the active site. Remarkably, this seemingly simple modification indeed provided a profound potency enhancement. Inhibitor **5**, a P1/P1' acylsulfonamide analogue, gave an IC_{50} of 2.2 nM, a boost of about 100 times over its carboxylic acid parent **4**. Its replicon EC_{50} of 17.5 nM was over 130 times more potent than **4**, although it is worth noting that the EC_{50}/IC_{50} ratio remained essentially unchanged as compared with its carboxylic acid counterpart.

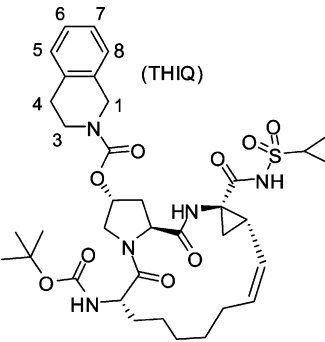
After intravenous administration to rats, inhibitor **5** was found to be rapidly cleared from the plasma compartment (clearance greater than blood flow). However, analysis of the animals' livers demonstrated excellent drug exposure and much lower clearance. This drastic tissue-specific clearance difference was again observed after the drug was orally administered to rats, and the compound's liver/plasma exposure ratio was greater than 1000.

Because HCV viral replication occurs predominantly, if not exclusively, in hepatocytes, excellent drug exposure in the liver (not plasma) should be a key predictor for sustained antiviral efficacy in patients. However, it was also observed that in vivo liver pharmacokinetics and [liver]/[plasma] ratios could range widely (>10 times), even among closely related analogues of **5**. Therefore, we resorted to systematically modifying various regions of lead molecule **5** to establish not only the structure–activity relationship, but the structure–pharmacokinetic relationship as well. With the newly obtained X-ray crystal structure

(Figure 1) in hand, we quickly focused on the following strategies for further lead optimization.

P2 Optimizations. As shown in Table 2, most of the substituted THIQ analogues did little to improve the replicon

Table 2. P2 THIQ Carbamate Inhibitory Activity against HCV NS3

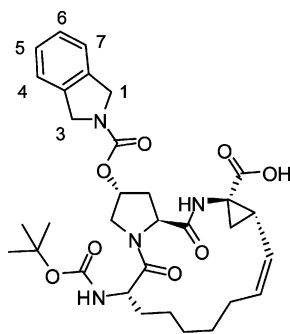


compd	THIQ	IC_{50} (nM)	EC_{50} (nM)
5	unsubstituted	2.2	18
28	4-OH	2.2	718
29	4-Me	1.0	5.7
30	4,4-dimethyl	0.8	7.7
31	5-F	0.7	12
32	5-NMe ₂	2.4	20
33	6-F	2.0	11
34	6-CF ₃	2.6	35
35	7-Cl	4.1	65
36	8-F	1.1	12
37	8-Cl	2.1	43
38	8-CF ₃	0.8	13
39	5,8-di-F	1.2	24

cell potency of the parent compound **5**. Efforts to block the likely metabolic site on the THIQ ring also failed to improve the compounds in vitro hepatic stability. Compounds **29** and **30** demonstrated a 3-fold improvement in replicon potency compared to **5**, but their hepatocyte stability was worse.

As described in Table 1, tetrapeptide analogue **27** bearing a P2 isoindoline carbamate was equipotent to **3** (IC_{50} = 186 and 210 nM, respectively), and the macrocyclic analogue of **3** maintained its potency (**4**, IC_{50} = 177 nM). However, the macrocyclic counterpart of **27** demonstrated an unexpected potency boost (**40**, Table 3, IC_{50} = 11 nM). It is plausible that isoindoline, a flatter ring system than THIQ, may enable better lipophilic interactions with the flat and lipophilic S2 protein surface. Further attempts to optimize the isoindoline group in this lead series via substitutions around the ring only yielded modest improvement (Table 3). Through these optimization efforts, isoindoline was identified as a more potent carbamate moiety than THIQ. Moreover, inhibitor **40** also enjoyed slower in vitro hepatic clearance and higher in vivo exposures in rats than its THIQ counterpart **4**. The lower hepatic clearance may be attributed to the elimination of the metabolically more vulnerable benzylic protons on the 4-position of the THIQ ring.

The superior potency of isoindoline over THIQ P2 carbamate was also clearly demonstrated in the macrocyclic P1/P1' acylsulfonamide series (Table 4). For instance, a 9-fold cell potency boost was observed comparing inhibitor **48** with **5** (EC_{50} = 2 vs 18 nM). Various substitutions around the isoindoline ring did not yield significant cell potency improvements, even though

Table 3. P2 Isoindoline Carbamate Inhibitory Activity against HCV NS3

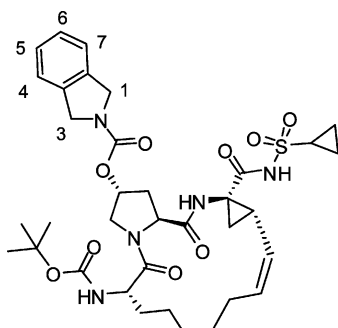
compd	isoindoline	IC ₅₀ (nM)	EC ₅₀ (nM)
40	unsubstituted	11	1550
41	4-Cl	13	516
42	4-F	10	1268
43	5-F	38	3220
44	5-CF ₃	195	7515
45	6-Cl	110	3159
46	5,6-di-Cl	483	25000
47	4,7-di-Cl	21	1475

the enzymatic potency of some of these new analogues was enhanced. Regardless of the steric or electronic nature of the substituents and their positions, nearly all the acylsulfonamide inhibitors tested in this series resulted in single-digit nanomolar enzymatic potency. Compound **55** was the only exception with an IC₅₀ value of 21 nM. Greater discrimination among the inhibitors was observed primarily in their cellular activities. Overall, single-point substitutions of small lipophilic groups, particularly at the 4-position of the isoindoline ring, resulted in the most active inhibitors in cells (**49**, **50**, **51**, **54**, **60**, and **61**). It is also worth noting that, because of the close proximity of the P3 cap and P2 parts of the inhibitor when bound to NS3 active site, an intramolecular interaction between the inhibitor's P2 and P3

cap moieties may have contributed to the inhibitor's overall binding affinity. However, it is not clearly understood why some of these inhibitors with equal or better enzymatic potency to inhibitor **48** lost much of their activity when tested in a cellular environment.

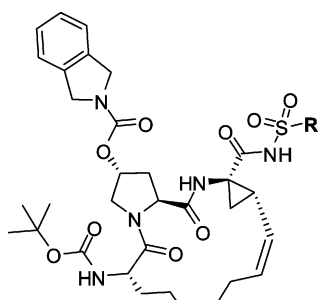
P1' Modifications. As shown in the X-ray crystal structure of **6** bound to the NS3 protease active site (Figure 1), the cyclopropyl P1' group appears to only partially fill the relatively large S1' pocket. Induced-fit computational docking suggested that larger groups such as phenyl rings might be better accommodated within the S1' site. Moreover, it is well-known in literature that amino acid residues in the NS3 S1' pocket demonstrate considerable conformational flexibility, producing an "induced fit" to accommodate a wide range of P1' substituent sizes. We investigated this by preparing a variety of P1/P1' aryl and alkyl acylsulfonamide analogues in an attempt to find an optimal motif that balances both potency and pharmacokinetic properties. For instance, switching from alkyl to aryl acylsulfonamides would not only adjust the P1' substituent's steric properties but would also modulate its acidity, thereby potentially affecting the overall pharmacokinetics of these new analogues. A number of these examples validated this approach and possessed comparable cell potency and rat pharmacokinetics to parent **48**. As shown in Table 5, small alkyl groups are tolerated in the P1' position up to the size of *tert*-butyl, which drastically diminished potency (**69**). Phenyl groups, on the other hand, were unexpectedly well tolerated even with para-substitutions, which appeared too large to fit in the S1' pocket in docking studies. This can be explained by examining the X-ray cocrystal structure of inhibitor **71**, which shows that the trajectory of the phenyl ring does not point toward the bottom of the S1' pocket as is the case for inhibitor **48** but is rather directed toward solvent.

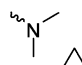
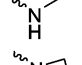

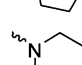
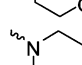
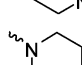
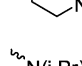
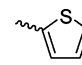
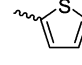
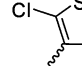
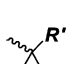
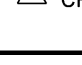
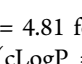
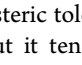
Acylsulfamides (**84–95**, Table 5) were introduced to further expand the scope of P1' region and explore possible DMPK benefits. Compared to its acylsulfonamide counterpart, acylsulfamide (or sulfonyl urea) was only slightly less acidic

Table 4. Inhibitory Activity against HCV NS3

compd	isoindoline	IC ₅₀ (nM)	EC ₅₀ (nM)	compd	isoindoline	IC ₅₀ (nM)	EC ₅₀ (nM)
48	unsubstituted	1.2	2.0	58	6-Cl	2.0	9.2
49	4-F	1.0	2.4	59	6-NH ₂	1.5	42
50	4-Cl	3	2.2	60	4,7-di-F	0.7	5.1
51	4-Br	1.1	49	61	4,7-di-Cl	1.7	7.3
52	4-CF ₃	1.2	29	62	5,6-di-Cl	1.0	24
53	4-NH ₂	0.2	4.1	63	5-morpholine	0.8	45
54	5-F	3	4.0	64	5-(N-Me-piperazine)	2.0	41
55	5-CF ₃	21	20	65	5-NH(iPr)	4.3	11
56	5-OCH ₃	2.3	22	66	4-morpholine	1.8	77
57	5-CN	2.5	112				

Table 5. P1' Inhibitory Activity SAR against HCV NS3



Cmpd	R	IC ₅₀ (nM)	EC ₅₀ (nM)	Cmpd	R	IC ₅₀ (nM)	EC ₅₀ (nM)
48	cyclopropyl	1.2	2.0	84		2.5	2.8
67	CH ₃	6.6	156	85		4.2	32
68	i-Pr	4.8	21	86		2.4	6.5
69	tert-Bu	37	194	87		2.6	11.8
70	CF ₃	4.8	166	88		4.4	52
71	C ₆ H ₅	3.5	11	89		22	509
72	p-Cl-C ₆ H ₅	3	58	90		17	46
73	p-MeO-C ₆ H ₅	4.1	10	91	N(i-Pr) ₂	70	139
74	p-CN-C ₆ H ₅	3	125	92	NH(C ₆ H ₅)	2.2	30
75	p-NMe ₂ -C ₆ H ₅	11	45	93	NH(p-Cl-C ₆ H ₅)	7.9	97
76	(2,5-di-F-C ₆ H ₅)	0.7	285	94	NH(p-MeO-C ₆ H ₅)	11	184
77		2.5	27	95	NH(p-CF ₃ -C ₆ H ₅)	9.8	70
78		4.6	111				
79		0.5	32				
80	 R' = CH ₃	0.5	3.1				
81	 R' = CH ₂ OCH ₃	7.7	13				
82	 R' = CH ₂ CH ₂ CH ₃	3	5				
83	 R' = CH ₂ Ph	1.6	25				

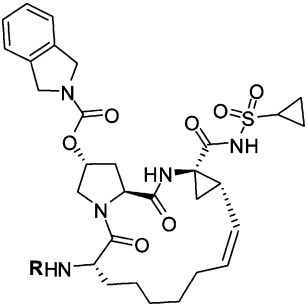
(e.g., ACD-predicted pK_a = 4.81 for **84**, and 4.49 for **48**), had very similar lipophilicity ($cLogP$ = 5.4 for both **48** and **84**), exhibited similar trend of steric tolerance for the P1' group and same level of potency, but it tended to show higher hepatic clearance rate as measured by in vitro hepatocyte stability assay (e.g., ER% = 1% and 16% for **48** and **84**, respectively, in rat hepatocytes).

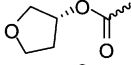
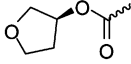
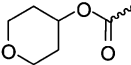
One of the most interesting changes observed in this series was some compounds' preferential tissue distributions to liver. For example, after orally dosed in rats, compound **48** had a liver/plasma ratio of approximately 1:1 throughout the time course (as measured by AUC_{0-24h}), whereas compound **84** displayed a liver/plasma ratio of >100:1 (Table 10). It was clear from this initial data that it would be almost impossible to use plasma concentration to predict whether the target organ (liver) would have adequate drug exposure, and that even seemingly small changes in drug design could result in drastically altering compound liver levels. Overall, on the basis of both EC_{50} and rat liver PK data, the optimal P1' group for this series were determined to be small lipophilic groups as in inhibitors **48**, **80**, and **84**.

P3 Cap Modifications. As our crystallographic studies illustrated, the P3 caps in the macrocyclic P2 carbamate

inhibitors interact with the S4 protein residues mainly through lipophilic interactions. A variety of modifications at this position are well tolerated in terms of maintaining their enzymatic potency (Table 6). Introduction of solubilizing groups into this region maintained enzymatic potency but resulted in a loss of cell potency (inhibitors **101**–**103**, Table 6). Switching the P3 cap from carbamate to urea improved the inhibitor's in vitro hepatic stability but lost about 10- to 20-fold cell activity (**99**, **100**).

Macrocyclic Linker Modifications. Reduction of the double bond on the macrocycle provided close-in analogues with slightly increased lipophilicity which sometimes improved cell potency. Unfortunately, the fully saturated aliphatic macrocycle linkers also tended to decrease the compounds' hepatic stability. Compounds in Table 7 exemplify our efforts to block potential metabolic sites on the macrocyclic linker. Reducing macrocyclic ring size from 15 to 14 resulted in a loss of cell potency (**105** vs **106** and **104** vs **49**). Replacing methylene groups on the 15-membered macrocycle with oxygen also significantly reduced cell potency (**49** vs **107**–**109**). In several examples, saturation of the double bond on the macrocyclic linker noticeably improved cell potency (**104** vs **105** and **107** vs **110**), but the alteration often led to deteriorated in vitro metabolic stability. Replacing a methylene with CF₂ did yield

Table 6. Inhibitory Activity SAR against HCV NS3 for P3 Caps


Cmpd	R	IC ₅₀ (nM)	EC ₅₀ (nM)
48	(t-Bu)O(CO)-	1.2	2
96	(cyclopentyl)O(CO)-	1	4
97	FCH ₂ CH ₂ O(CO)-	1.5	54
98	CF ₃ CH ₂ CH ₂ O(CO)-	0.6	48
99	(t-Bu)NH(CO)-	2.4	38
100	(cyclopentyl)NH(CO)-	0.7	26
101		2.8	107
102		2.2	217
103		2.2	97

analogues with the same level of replicon potency as parent **49** (**113** and **118**). Unfortunately, none of these analogues that were designed to reduce metabolic soft spots actually improved in vitro metabolic stability or in vivo exposures in rats.

P2 Linker Modifications. A variety of P2 linkers besides carbamate were prepared based on the X-ray crystal structure of inhibitor **6** bound to the NS3 active site. The enzymatic and cellular activities of these analogues are shown in Table 8. Analogues with a sulfonamide linker (e.g., **122**) demonstrated a significant loss of enzymatic potency, whereas analogues with an amide or a urea linker maintained the same level of enzymatic potency as the carbamate-linked inhibitors. Certain amide-linked inhibitors such as **126** and **127** showed the least cell potency loss but were still 5–10-fold less potent than **49**.

In summary, potent antiviral activity of this novel class of macrocyclic NS3 protease inhibitors was achieved through optimization of the P1', P2, and P3 groups (Table 9). Individually, either a flat bicyclic lipophilic ring at P2 or a small alkyl acylsulfonamide at P1/P1' brought a similar magnitude of EC₅₀ enhancement, from inactive (**130**) to ~2 μM (**4**, **40**, and **131**). Taken together, the two modifications further improved the EC₅₀ to <20 nM (**5**, **48–50**). Attempts to trim the high molecular weights of these macrocyclic peptidomimetics at the P2 or P4 position generated inhibitors with good enzymatic activity (IC₅₀ < 20 nM) but with seriously eroded cell potency (**133–136**).

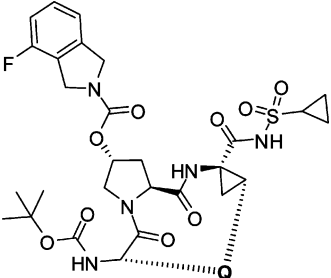
Preclinical Development. After investigation of the DMPK profiles of this new class of NS3 inhibitors, numerous candidates emerged as having both the desired replicon potency and excellent in vivo liver exposures in multiple animal species after oral dosing. The drug distribution between plasma and the target organ liver varied drastically even among very close-in analogues,

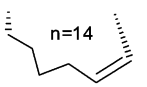
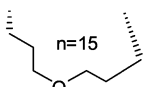
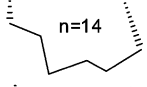
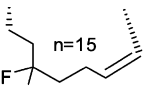
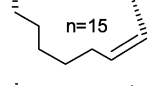
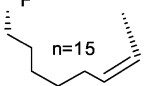
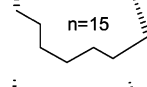
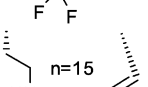
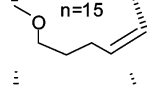
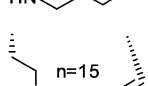
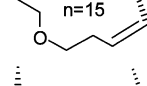
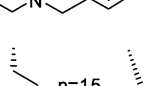
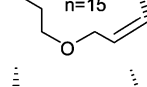
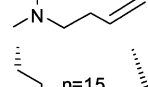
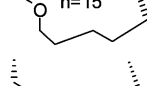
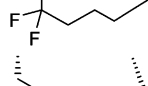
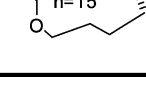
from approximately 1:1 to >4000:1 (Table 10). The significantly different liver preference displayed by these inhibitors probably have much to do with their different affinities to active uptake and efflux transporters in addition to their physicochemical properties.¹⁸ Given their excellent antiviral potency and good range of preferential liver distribution, inhibitors **49** and **84** were selected as preclinical candidates for animal safety studies. On the basis of the overall safety study results, compound **49** was selected as the clinical development candidate. The preclinical profile of **49** is summarized in Figure 2.¹⁷ Detailed discussions of its preclinical characteristics including pharmacokinetics in rodents and cynos have been disclosed elsewhere.^{9a}

X-ray Crystal Structure. An X-ray crystal structure of danoprevir bound in HCV NS3 protease was determined in-house at 2.7-Å resolution by soaking the inhibitor into an apo-structure of the enzyme that was solved earlier in the program. This effort revealed a unique, noncovalent binding mode for danoprevir, distinct from the binding modes observed for covalent inhibitors telaprevir and boceprevir.^{7,8} As shown in Figures 3 and 4, the S1/S1' pocket is occupied by the cyclopropyl acylsulfonamide, with the acyl carbonyl oxygen projecting deep in the oxyanion hole of the protease active site as it makes hydrogen bonds to Gly137 and Ser138. The sulfonyl oxygens make hydrogen bonds with Gly137 and Ser139, while the nitrogen of the acyl sulfonamide makes a hydrogen bond with His57. It is postulated that the acyl sulfonamide exists as an anion when bound, with His57 being protonated when hydrogen-bonding to the acyl nitrogen. The P2 fluoroisindoline lies in a lipophilic portion of the extended S2 pocket with the fluorine directed toward the P3 *tert*-butyl carbamate cap, which in turn occupies the shallow S4 pocket. The aliphatic chain linking the P1 cyclopropyl to the P3 position lies in a deep hydrophobic cleft extending from the S1 to S3 sites. The extraordinary inhibitory potency observed for danoprevir arises from the highly optimized and synergistic combination of its tight hydrogen-bonding network in the S1/S1' site along with the extensive van der Waals interactions within the S1–S3 lipophilic cleft and along the extended S2 pocket.

Recently, a crystal structure of danoprevir in complex with wild-type NS3 protease (PDB ID 3MSL) was reported by an independently conducted research.^{19a} It is of higher resolution than our previously undisclosed in-house structure, but the inhibitor binding conformation and protein residue coordinates reported are in good agreement with what we have observed. One difference is that in this recent report two conformations of danoprevir's isindoline P2 moiety were observed (with fluorine either facing or 180° facing away from the P3 cap), whereas we had only observed one conformation (with fluorine facing the P3 cap). The existence of two danoprevir P2 conformations is not completely unexpected, considering their being nearly equilibrium rotamers.

Danoprevir Still Potent Against A156T Resistance Mutation. In the crystal structure of danoprevir bound to wild-type NS3 protease (Figure 3), the methyl group side chain of Ala 156 projects upward and is surrounded by the P2 fluoroisindoline and the *tert*-butyl carbamate of the P3 cap. In the presence of the drug-resistant A156T mutation, telaprevir loses >100-fold potency and becomes essentially inactive, while both ciluprevir and vaniprevir lose >1000-fold of their potency.^{15,19b} Danoprevir, on the other hand, only experiences a ~2-fold drop in potency (from <0.25 to 0.50 nM).²¹ Our docking studies predict that danoprevir should be accommodated in the A156T resistant mutant protease for two reasons.

Table 7. Inhibitory Activity SAR against HCV NS3 for Various Macrocyclic Linkers^{a,b}


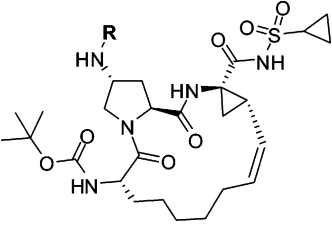
Cmpd	Q	IC ₅₀ (nM)	EC ₅₀ (nM)	Cmpd	Q	IC ₅₀ (nM)	EC ₅₀ (nM)
104		1.5	76.6	112		1.0	254
105		1.5	22.5	113		1.5	7.2
49		1.0	2.4	114		0.5	44
106		0.7	5.8	115		9.7	1827
107		1.8	70.2	116		1.8	24
108		1.2	33	117		7.0	837
109		0.8	155	118		0.8	6.8
110		1.2	12.4	119		1.3	46
111		0.7	19				

^aThe *n* values herein refer to the macrocyclic analogue's overall ring size. ^bThe syntheses for inhibitors listed in this table can be found in Supporting Information.

First, unlike the large P2 group present in ciluprevir, the P2 isoindoline group of danoprevir can undergo significant movement in the presence of T156 without creating additional steric clashes in the extended S2 pocket. Second, relative to telaprevir and vaniprevir, the inherent rotational flexibility in the P2 and P3 cap carbamate linkage of danoprevir allows it to undergo movements to avoid steric clashes with T156. These features are illustrated in the docking of danoprevir into an A156T mutant HCV NS3 protease generated *in silico* and energy-minimized for the lowest energy rotamer of residue T156. The relatively flexible P2 and P3 cap substituents of danoprevir ease apart and twist slightly to accommodate the larger T156 residue (Figure 5).

Romano et al. have recently reported a crystal structure of danoprevir in complex with A156T mutant NS3 protease (PDB ID 3SU2).^{19b} The inhibitor binding conformation and protein

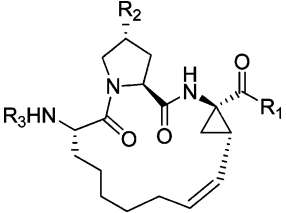
residue positions observed are in good agreement with what we had anticipated from docking studies. One difference is that we have previously hypothesized the possibility for the P2 fluoroisoindoline to rotate 180° (with the fluorine facing away from the P3 cap) to further alleviate steric clashes with T156. Both conformations were indeed reported for danoprevir in complex with wild-type NS3 protease as aforementioned. However, only a single P2 isoindoline conformation was observed in this mutant structure (with the fluorine facing the P3 cap). This is likely a result of danoprevir's flexible P2 group making compensatory packing against the larger T156 side chain after shifting apart from the P3 cap, therefore retaining its potency against the mutant. Other common resistance mutations observed in the clinic during danoprevir monotherapy (e.g., R155K) have been reported elsewhere.²⁰

Table 8. Inhibitory Activity SAR against HCV NS3:P2 Noncarbamate Linkers^a


Cmpd	R	IC ₅₀ (nM)	EC ₅₀ (nM)	Cmpd	R	IC ₅₀ (nM)	EC ₅₀ (nM)
120		2.9	362	125		1.4	21
121		2.3	47	126		1.4	9.5
122		470	>10,000	127		3.5	13
123		8.2	365	128		5.2	126
124		21	730	129		6.4	614

^aThe syntheses for inhibitors listed in this table can be found in Supporting Information.

Table 9. Inhibitory Activity SAR against HCV NS3



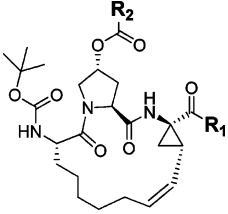
compd	R1	R2	R3	IC ₅₀ (nM)	EC ₅₀ (nM)
130	OH	OH	Boc	>50000	NA
4	OH	O(CO)(THIQ)	Boc	177	2352
40	OH	O(CO)(isoindoline)	Boc	11	1550
131	NHSO ₂ (cyclopropyl)	OH	Boc	75	2131
132	NHSO ₂ (cyclopropyl)	OMe	Boc	220	6300
133	NHSO ₂ (cyclopropyl)	OAc	Boc	12	3913
134	NHSO ₂ (cyclopropyl)	OBu'	Boc	3	91
5	NHSO ₂ (cyclopropyl)	O(CO)(THIQ)	Boc	2	18
48	NHSO ₂ (cyclopropyl)	O(CO)(isoindoline)	Boc	1	2
49	NHSO ₂ (cyclopropyl)	O(CO)(4'-F-isoindoline)	Boc	1	2
135	NHSO ₂ (cyclopropyl)	O(CO)(4'-F-isoindoline)	H	20	3050
50	NHSO ₂ (cyclopropyl)	O(CO)(4'-Cl-isoindoline)	Boc	3	2
136	NHSO ₂ (cyclopropyl)	O(CO)(4'-Cl-isoindoline)	H	3	150

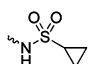
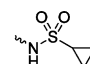
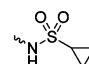
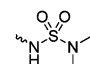
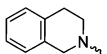
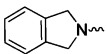
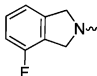
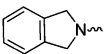
CONCLUSIONS

Through structure-based design and optimization, a new class of macrocyclic peptidomimetic NS3/4A protease inhibitors has been discovered. A virtual chemical library of approximately 500 molecules was designed and screened using a unique docking hypothesis that was established on the basis of analyzing NS3 X-ray crystallographic structures and carefully studying the

resulting binding modes predicted by docking. On the basis of these virtual screening studies, tetrapeptides with a P1/P1' carboxylic acid headgroup and P2 carbamates extending from a hydroxyproline were selected as lead-generation chemical targets. A facile chemistry route was then identified to couple hydroxyproline with various amine inputs, which enabled efficient modifications of the P2 substituent. Initial P2 SAR

Table 10. ADME/PK Profiles of Danoprevir and Close Analogues



Cmpd	5	48	49	84
R1				
R2				
cLogP / LogD / tPSA	5.9 / 2.2 / 180	5.4 / 2.4 / 180	5.6 / 2.1 / 180	5.4 / 2.5 / 184
IC ₅₀ / EC ₅₀ (nM)	2 / 18	1 / 2	1 / 2	1 / 3
Hepatocytes Stability ^a ER% (human/rat/cyno/ dog)	49 / 5 / 53 / 36	65 / 1 / 28 / 33	58 / 6 / 54 / 23	56 / 16 / 56 / 16
Solubility (μg/mL) ^b @pH 1.2 / 6.5 / 7.4	0.5 / 812 / >1000	0.5 / 702 / >1000	0.5 / 548 / >1000	0.5 / 165 / >1000
Caco Permeability ^c	low / efflux	low / efflux	low / efflux	low / efflux
Plasma CL (ER%) ^d	> 100%	6 %	4 %	> 100%
V _{ss} (mL/kg) ^d	5,982	89	155	2,583
Liver AUC _{0-24h} (μg*h/mL) ^e	276.5	40.3	90.8	136.3
Plasma AUC _{0-24h} (μg*h/mL) ^e	0.06	32.9	9.5	1.03
AUC _{liver} / AUC _{plasma}	4608	1.2	10	132

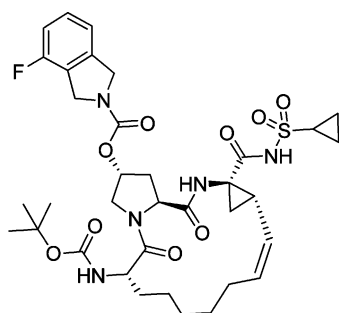
^aTest article concentration = 1 μM. ^bTested in aqueous pH buffers. ^cTest article's permeability is reported as "low" when $Pe_{AB} < 2 \times 10^{-6}$ cm/s, and "efflux" indicates Pe_{BA}/Pe_{AB} ratio >2. ^dRat, 1 mg/kg, IV ER% = $CL_{obs}/(\text{hepatic blood flow rate})$; Both CL_{obs} and blood flow rate are expressed in mL/min/kg, and 70 mL/min/kg blood flow rate was used to calculate rat plasma clearance values; ^eRat, 30 mg/kg, PO cohorts of three animals were sacrificed for each time point of the liver PK.

trends gleaned from this tetrapeptide carbamate series focused our attention on several preferred structures that were all relatively flat and rigid. Compound **3** (Scheme 1), which features a tetrahydroisoquinoline (THIQ) carbamate motif, became our first lead. However, the lack of cellular potency of **3** necessitated additional modifications, which led to the transformation of tetrapeptide lead **3** to macrocyclic lead **4**. Further modification of the P1/P1' carboxylic acid headgroup to acylsulfonamide resulted in inhibitor **5**, which showed a profound potency boost in both enzymatic and cellular assays, with the latter <20 nM.

Pharmacokinetic results of selected inhibitors in rats revealed a wide range of drug exposures in the target tissue (liver), and drug concentrations in plasma were often not indicative of their liver levels. In fact, the ratio between drug concentrations in liver and plasma could easily vary more than 2 orders of magnitude even among highly similar analogues.^{13a} We systematically examined

both the structure–activity relationship and the structure–pharmacokinetics relationship in key regions of lead **5** in order to optimize both potency and PK properties. These efforts led to the discovery of compound **49**, which exhibited low nanomolar potency in replicon cells and efficacious liver exposures in rats and monkeys (30 mg/kg, PO).^{9a}

Our X-ray crystal structure of **49** bound to NS3 illustrated distinctive binding features of the inhibitor to the NS3 active site that support the enzyme kinetic analysis results of a noncovalent inhibitor with a slow/tight binding mechanism that is associated with slow dissociation.^{9a,13b} Compound **49** (danoprevir) is currently undergoing phase II clinical trials and has demonstrated robust antiviral efficacy in patients with chronic HCV infections.



49 (ITMN-191, R7227)

M.W. = 731.8, cLogP = 5.6, LogD = 2.1
 pKa = 5.27 (ACD pred. 4.47)
 m.p. = 137.3 °C
 IC₅₀ = 0.2–0.4 nM (1a, 1b, 4, 5 & 6), 1.6 nM (2b),
 3.5 nM (3a)
 EC₅₀ = 1.6 nM (1b), 20 nM (2 & 3)
 MT4-MTT CC₅₀ = 54 μM
 CYP 1A2, 2C19, 2C9, 2D6 > 25 μM; 3A4 = 12 μM
 Time-dependent CYP3A4 inhibition/induction: Negative
 hERG %block @ 10 μM: Negative
 Selectivity: IC₅₀ > 10 μM in panel of 53 proteases
 Oral bioavailability (liver): 15 % (rat); 78 % (monkey)
 Liver/plasma ratio: ~10 (rat); ~30 (dog); ~100 (monkey)

Figure 2. Danoprevir preclinical data profile.

EXPERIMENTAL SECTION

The reactions described herein were generally conducted under a positive pressure of nitrogen or argon or with a drying tube in commercial anhydrous solvents unless otherwise stated, and the reaction flasks were typically fitted with rubber septa during the introduction of reagents via a syringe or cannula. Glasswares were oven and/or heat dried. All reagents and solvents were used without further purification unless otherwise stated. Reaction progress was monitored by analytical TLC, HPLC, and LCMS. Analytical TLC was performed using glass plates precoated with silica gel from EMD (60 F₂₅₄, 250 μm). TLC visualization was performed with UV light or by staining with Hanessian's stain or basic KMnO₄ solution. Flash column chromatography was performed on a Biotage model SP1 purification system

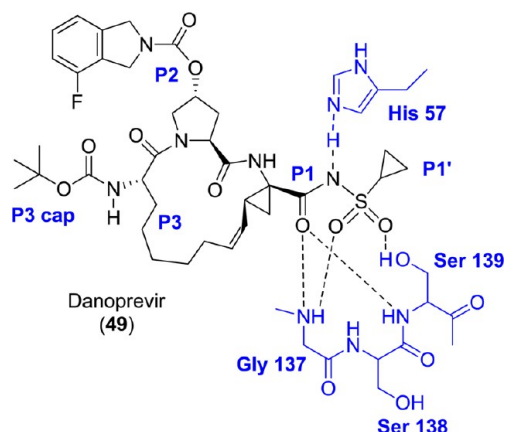


Figure 4. Unique binding mode of danoprevir (49) to NS3 protease active site maximizes potency.

running SPX software with prepacked silica gel or C18 columns and UV detection at 220 and 254 nm. Analytical HPLC was performed on an Agilent 1200 (column YMC ODS-AQ 3 μm, 120 Å, 3.0 mm × 50 mm; run gradient 5–95% 0.01% HFBA/1% IPA/water/acetonitrile; UV detection 220 and 254 nm). Analytical LCMS was performed on an Agilent 1200 HPLC coupled with an Agilent 6120 quadrupole LC/MS spectrometer using ESI or APCI ionization sources (column YMC ODS-AQ 4.6 mm × 50 mm, 3 μm, 120 Å; run gradient 5–95% B over 4.5 min, holding 95% B for 1 min, followed by equilibration for 1 min; flow rate 2 mL/min; solvent A water/10 mM ammonium acetate/1% IPA; solvent B acetonitrile/10 mM ammonium acetate/1% IPA). Melting points were recorded on an electrothermal melting point apparatus, model 9100. ¹H NMR spectra were recorded in CDCl₃, acetone-*d*₆ or DMSO-*d*₆ solvents on a Varian Mercury (400 MHz) NMR spectrometer or on a Bruker AV III (400 or 500 MHz) spectrometer. Chemical shifts are expressed in parts per million (ppm, δ scale) using tetramethylsilane as the reference standard. When peak multiplicities are reported, the following abbreviations are used: s (singlet), d (doublet), t (triplet), q (quartet), m (multiplet), dd (doublet of doublet), dt (doublet of triplet), br (broad). Coupling constants are reported in hertz (Hz). The purity of each compound that was synthesized and tested for biological activity was ≥95% via HPLC analysis.

(2*R*,6*S*,13*aS*,14*aR*,16*aS*,*Z*)-6-(*tert*-Butoxycarbonylamino)-5,16-dioxo-2-(1,2,3,4-tetrahydroisoquinoline-2-carboxyloxy)-

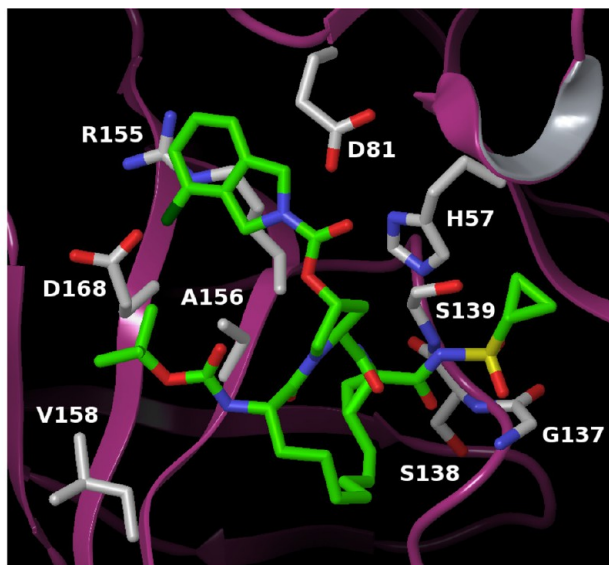
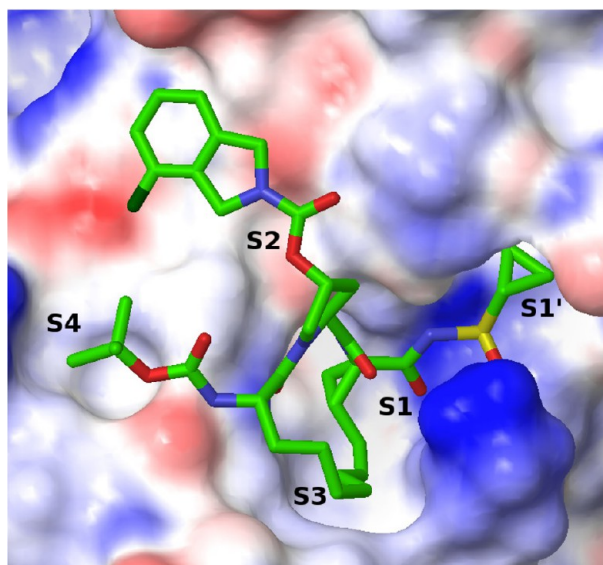


Figure 3. X-ray crystal structure of danoprevir (49) bound to NS3 protease active site.

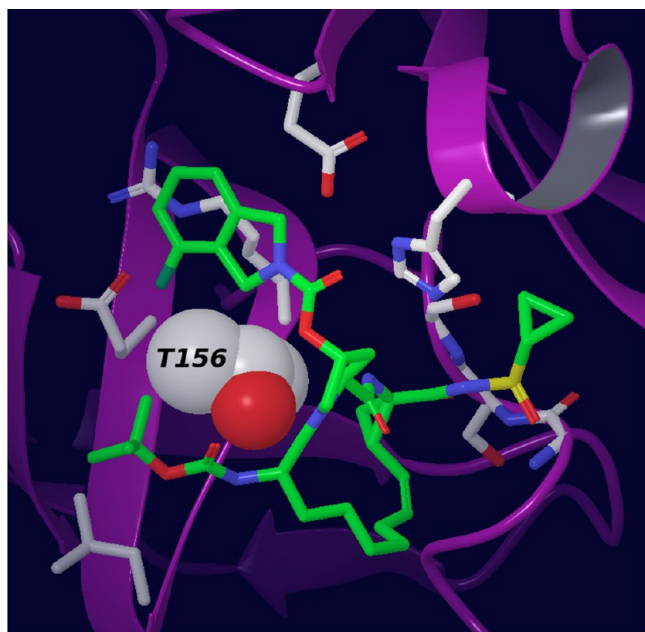


Figure 5. Danoprevir docked into A156T mutant HCV NS3 protease (T156 shown as space-filling representation).

1,2,3,5,6,7,8,9,10,11,13a,14,14a,15,16,16a-hexadecahydrocyclopropa[e]pyrrolo[1,2-a][1,4]-diazacyclopentadecine-14a-carboxylic Acid (4). The macrocyclic intermediate **13** (110 mg, 0.22 mmol) was dissolved in DCM (2.2 mL), followed by addition of CDI (45 mg, 0.27 mmol) in one portion. The reaction was stirred at room temp overnight. After 15 h, 1,2,3,4-tetrahydroisoquinoline (0.14 mL, 1.1 mmol) was added to the reaction dropwise, and the reaction was stirred at room temp overnight. After 22 h, the reaction was diluted with DCM (6 mL) and washed with 1N aq HCl (2 × 2 mL), satd NaHCO₃ (2 mL), and brine (2 mL), and then dried (Na₂SO₄), filtered, and concentrated. The crude was purified on silica Biotage system (2 to 4% MeOH in DCM), giving **14** as a pale-yellowish foamy powder (131 mg, 90%).

The macrocyclic ester **14** (60 mg, 0.092 mmol) was dissolved in 0.9 mL of a mixture solvent (THF/MeOH/H₂O 2:2:1), followed by addition of LiOH·H₂O (23 mg, 6 equiv). The mixture was stirred at room temp overnight. After 18 h, the reaction was concentrated down to near dryness and partitioned between 1N aq HCl (15 mL) and DCM (20 mL). The aqueous layer was extracted with DCM (2 × 10 mL). The organic layers were combined, dried over Na₂SO₄, and concentrated down, giving **4** as a light-brownish foamy powder (50 mg, 87%). ¹H NMR (CD₃OD, 400 MHz) δ 1.20–1.67 (m, 21 H), 1.70–1.83 (m, 1 H), 1.88–2.10 (m, 1 H), 2.12–2.58 (m, 4 H), 2.82 (m, 2 H), 3.60–3.80 (m, 2 H), 3.86 (m, 1 H), 4.20 (m, 1 H), 4.35 (m, 1 H), 4.54 (s, 7 H), 4.58 (m, 3 H), 5.29–5.41 (m, 2 H), 5.57 (m, 1 H), 7.0–7.24 (m, 4 H). MS *m/z* 625.1 (M⁺ + 1).

(2R,6S,13aS,14aR,16aS,Z)-6-(tert-Butoxycarbonylamino)-14a-(cyclopropylsulfonylcarbonyl)-5,16-dioxo-1,2,3,5,6,7,8,9,10,11,13a,14,14a,15,16,16a-hexadecahydrocyclopropa[e]pyrrolo[1,2-a][1,4]-diazacyclopentadecin-2-yl 3,4-dihydroisoquinoline-2(1H)-carboxylate (5). The macrocyclic acid **4** (197 mg, 0.32 mmol) was dissolved in 3 mL of DMF, followed by addition of CDI (76.7 mg, 0.47 mmol). The mixture was stirred at 50 °C for 2 h. After cooling back to room temperature, cyclopropylsulfonamide (57.3 mg, 0.47 mmol) was added in one portion, followed by DBU (72 mg, 0.47 mmol). Heating was then resumed, and the reaction was stirred at 50 °C for 1 h to reach completion. After removal of solvent, the crude product was purified by silica chromatography on the Biotage system (40% EtOAc/hexanes with 1% formic acid), giving **5** as a white foamy solid (216 mg, 94%). ¹H NMR (CDCl₃, 500 MHz): δ 0.80–2.10 (m, 25 H), 2.20–2.27 (m, 1 H), 2.37–2.59 (m, 3 H), 2.84 (m, 1 H), 3.60–3.70 (m, 1 H), 3.82–3.90 (m, 1 H), 4.20–4.30 (m, 2 H), 4.45–4.70 (m, 5 H), 4.95–5.05 (m, 2 H),

5.30–5.48 (m, 2 H), 5.74 (m, 1 H), 6.74 (m, 1 H), 7.0–7.23 (m, 4 H). MS *m/z* 728.0 (M⁺ + H).

(2S,4R)-tert-Butyl 2-((trans)-1-(Ethoxycarbonyl)-2-vinylcyclopropylcarbonyl)-4-hydroxypyrrolidine-1-carboxylate (8). A solution of (2S,4R)-1-(tert-butoxycarbonyl)-4-hydroxypyrrolidine-2-carboxylic acid (2.52 g, 10.9 mmol), (trans)-ethyl 1-amino-2-vinylcyclopropanecarboxylate hydrochloride (2.30 g, 12.0 mmol), and HATU (4.56 g, 12.0 mmol) in 50 mL of DMF was cooled to 0 °C. DIEA (7.60 mL, 43.6 mmol) was added dropwise as a solution in 20 mL of DMF, and the reaction was allowed to warm to room temperature overnight. The solution was partitioned between EtOAc and water, and the organic layer was washed 2× with water, 0.1N HCl, and brine, dried over Na₂SO₄, and concentrated. The crude was purified by silica chromatography (3–5% MeOH/DCM) to give Boc-dipeptide **8** as a white foamy solid (3.3 g, 81%). ¹H NMR (400 MHz, acetone-*d*₆) δ 7.95–7.98 (m, 1H), 5.68–5.78 (m, 1H), 5.20–5.27 (m, 1H), 5.04–5.07 (m, 1H), 4.43 (br s, 1H), 4.20–4.28 (m, 2H), 4.01–4.16 (m, 2H), 3.40–3.53 (m, 2H), 3.30 (br s, 1H), 2.05–2.25 (m, 3H), 1.68–1.78 (m, 1H), 1.41 (s, 9H), 1.20 (t, 3H, *J* = 7.0 Hz). MS (ES) *m/z*: 391.1 (M + Na⁺).

(2S,4R)-tert-Butyl 2-((1R,2S)-1-(Ethoxycarbonyl)-2-vinylcyclopropylcarbonyl)-4-hydroxypyrrolidine-1-carboxylate (8b). To a flask charged with ethyl-(1R,2S)-1-amino-2-vinylcyclopropyl carboxylate (1.0 g, 5.2 mmol), (2S,4R)-1-(tert-butoxycarbonyl)-4-hydroxypyrrolidine-2-carboxylic acid (1.3 g, 1.1 equiv), and HATU (2.7 g, 1.1 equiv) were added 30 mL of DMF to make a solution. It was cooled to 0 °C in an ice–water bath, followed by slow addition of a solution of DIEA (4.4 mL, 4 equiv) in DMF (15 mL) while stirring. The reaction was allowed to warm up to ambient temperature and stirred overnight. After 16 h, the reaction was diluted with EtOAc (100 mL), washed with water (3 × 40 mL), satd NaHCO₃ (2 × 40 mL), and brine (2 × 40 mL), and then dried over anhydrous Na₂SO₄ and concentrated. The crude was purified on silica gel (acetone/hexanes 3:7), giving pure desired product as beige foamy powder (770 mg, 32%). MS (ES) *m/z*: 391.1 (M + Na⁺).

(trans)-Ethyl 1-((2S,4R)-1-((S)-2-(tert-Butoxycarbonylamino)-3-methylbutanoyl)-4-hydroxypyrrolidine-2-carboxamido)-2-vinylcyclopropanecarboxylate (9). The crude dipeptide **8** was dissolved in 50 mL of 4N HCl/dioxane and stirred at room temperature for 25 min. The volatiles were removed by rotary evaporation giving an oil which was dissolved in 200 mL of acetonitrile and concentrated to give **8a** as an orange foam. A solution of **8a**, (S)-2-(tert-butoxycarbonylamino)-3-methylbutanoic acid (2.94 g, 13.5 mmol), and HATU (5.14 g, 13.5 mmol) in 70 mL of DMF was cooled to 0 °C. DIEA (8.57 mL, 49.2 mmol) was added dropwise as a solution in 20 mL of DMF, and the reaction was warmed to room temperature overnight. The solution was partitioned between EtOAc and water, and the organic layer was washed 2× with water, 0.1N HCl, and brine, dried over Na₂SO₄, and concentrated to give Boc-tripeptide **9** as a brown oil which was used in the next step without further purification. MS (ES) *m/z*: 490.2 (M + Na⁺).

(trans)-Ethyl 1-((2S,4R)-1-((S)-2-((S)-2-(tert-Butoxycarbonylamino)-2-cyclohexylacetamido)-3-methylbutanoyl)-4-hydroxypyrrolidine-2-carboxamido)-2-vinylcyclopropanecarboxylate (10a). The crude tripeptide **9** (5.7 g, 12.3 mmol) was dissolved in 50 mL of 4N HCl/dioxane and stirred at room temperature for 25 min. The volatiles were removed by rotary evaporation, giving an oil which was dissolved in 200 mL of acetonitrile and concentrated to give **9a** as an orange foam. A solution of **9a**, (S)-2-(tert-butoxycarbonylamino)-2-cyclohexylacetic acid (3.48 g, 13.5 mmol), and HATU (5.13 g, 13.5 mmol) in 70 mL of DMF was cooled to 0 °C. DIEA (8.57 mL, 49.2 mmol) was added dropwise as a solution in 20 mL of DMF, and the reaction was warmed to room temperature overnight. The solution was partitioned between EtOAc and water. After phase separation, the organic layer was washed with water, NaHCO₃ (satd), and brine (100 mL each), dried over Na₂SO₄, and then concentrated. The crude was purified by silica gel flash chromatography (3–5% MeOH in DCM) to give Boc-tetrapeptide **10a** as a white foamy solid (4.4 g, 59%). MS (ES) *m/z*: 629.2 (M + Na⁺).

(1S,2R)-Ethyl 1-((2S,4R)-1-((S)-2-((S)-2-Acetamido-2-cyclohexylacetamido)-3-methylbutanoyl)-4-hydroxypyrrolidine-2-carboxamido)-2-vinylcyclopropanecarboxylate (10). The crude

tetrapeptide **10a** (4.42 g, 7.28 mmol) was dissolved in 50 mL of 4N HCl/dioxane and stirred at room temperature for 45 min. The volatiles were removed by rotary evaporation, giving an oil which was dissolved in 200 mL of acetonitrile and concentrated to give deprotected **10a** as an orange foam. A solution of the deprotected **10a**, acetic acid (0.46 mL, 8.01 mmol), and HATU (3.05 g, 8.01 mmol) in 70 mL of DMF was cooled to 0 °C. DIEA (5.08 mL, 29.1 mmol) was added dropwise as a solution in 20 mL of DMF, and the reaction was warmed to room temperature overnight. The solution was partitioned between EtOAc and water. After phase separation, the organic layer was washed with water, NaHCO₃ (satd), and brine (100 mL each), dried over Na₂SO₄, and concentrated. The crude was purified by silica gel flash chromatography (3–5% MeOH in DCM) to give **10** as a white foamy solid (2.38 g, 60%). ¹H NMR (400 MHz, acetone-*d*₆) δ 11.25 (bs, 1H), 8.17–8.27 (m, 1H), 7.72 (br s, 1H), 7.12–7.29 (m, 1H), 7.17 (s, 1H), 5.72–5.85 (m, 1H), 5.37 (br s, 1H), 5.22–5.32 (m, 1H), 5.05 (d, 1H, *J* = 10.1 Hz), 4.35–4.64 (m, 5H), 4.15–4.24 (m, 1H), 3.90–4.00 (m, 1H), 3.63 (br s, 1H), 2.33–2.40 (m, 1H), 2.19 (m, 1H), 2.03–2.13 (m, 1H), 1.91–1.99 (m, 4H), 1.50–1.77 (m, 7H), 1.40–1.47 (m, 1H), 0.86–1.23 (m, 12H). MS (ES) *m/z*: 571.4 (M + Na⁺).

(1R,2S)-Ethyl 1-((2S,4R)-1-((S)-2-(tert-butoxycarbonylamino)non-8-enoyl)-4-hydroxypyrrolidine-2-carboxamido)-2-vinylcyclopropanecarboxylate (12). Compound **8b** (2.85 g, 7.7 mmol) was first stirred in HCl (10 mL × 4N, dioxane) at room temp for 90 min. After removal of solvent on rotary evaporator and then high vacuum, (S)-2-(tert-butoxycarbonylamino)non-8-enoic acid (**11**) (2.2 g, 8.1 mmol) and HATU (3.2 g, 8.5 mmol) were added, followed by DMF (80 mL). The reaction mixture was cooled to 0 °C, then 5 mL of DMF solution of DIEA (5.4 mL, 30.9 mmol) was added to the reaction dropwise while stirring. The reaction was allowed to warm up to room temp and stirred overnight. After 18 h, the reaction was diluted with EtOAc (300 mL) and washed with water (3 × 150 mL), satd NaHCO₃ (2 × 150 mL), and brine (150 mL), dried over anhydrous Na₂SO₄, filtered, and concentrated. The crude was purified by silica gel flash chromatography on Biotage (3–5% MeOH in DCM) to give **12** as a brownish foamy solid (3.5 g, 87%). ¹H NMR (benzene-*d*₆, 400 MHz) δ 0.87 (t, *J* = 5.2 Hz, 3H), 1.34 (s, 9H), 1.10–1.31 (m, 8H), 1.36–1.46 (m, 1H), 1.65–1.74 (m, 1H), 1.80–1.94 (m, 4H), 2.00–2.09 (m, 1H), 2.28–2.35 (m, 1H), 3.18 (dd, 1H, *J* = 11.2 and 4.8 Hz), 3.54 (bd, 1H, *J* = 11.2 Hz), 3.80–3.86 (m, 1H), 3.89–3.97 (m, 1H), 4.14 (br s, 1H), 4.34–4.42 (m, 1H), 4.63 (t, 1H, *J* = 7.2 Hz), 4.91–5.00 (m, 3H), 5.17 (d, 1H, *J* = 16.8 Hz), 5.32 (bd, 1H, *J* = 7.6 Hz), 5.66–5.77 (m, 1H), 5.80–5.89 (m, 1H), 7.59 (br s, 1H). ¹³C NMR (benzene-*d*₆, 100 MHz) δ 172.9, 171.4, 169.9, 156.1, 138.9, 134.2, 117.4, 114.4, 79.6, 70.2, 60.9, 58.5, 55.1, 52.5, 40.3, 35.9, 33.8, 33.7, 32.5, 29.0, 28.9, 28.2, 25.2, 23.0, 14.1. MS *m/e* 522.3 (M⁺ + 1).

(2R,6S,13aS,14aR,16aS,Z)-Ethyl 6-(tert-butoxycarbonylamino)-2-hydroxy-5,16-dioxo-1,2,3,5,6,7,8,9,10,11,13a,14,14a,15,16,16a-hexadecahydrocyclopropa[e]pyrrolo[1,2-a][1,4]diazacyclopentadecine-14a-carboxylate (13). A solution of compound **12** (2.6 g, 5.0 mmol) in dry DCE (500 mL) was first degassed by bubbling through nitrogen for 1 h before Hoveyda's first-generation catalyst (0.25 equiv) was added in one portion. The reaction was then stirred at 50 °C under nitrogen atmosphere overnight. After 16 h, the reaction was concentrated on rotary evaporator and purified on silica Biotage system (DCM/EtOAc 1:1 to 1:2), giving **13** as a beige foamy powder (0.64 g, 52%). ¹H NMR (CDCl₃, 400 MHz) δ 1.21 (t, *J* = 7.0 Hz, 3H), 1.43 (s, 9H), 1.20–1.50 (m, 6H), 1.53–1.68 (m, 2H), 1.83–1.96 (m, 2H), 1.98–2.28 (m, 4H), 2.60 (m, 1H), 3.13 (br s, 1H), 3.68 (m, 1H), 3.94 (m, 1H), 4.01–4.19 (m, 2H), 4.48 (m, 1H), 4.56 (br s, 1H), 4.79 (m, 1H), 5.26 (t, *J* = 9.4 Hz, 1H), 5.36 (d, *J* = 7.8 Hz, 1H), 5.53 (m, 1H), 7.19 (br s, 1H). MS *m/e* 494.0 (M⁺ + 1).

(2R,6S,13aS,14aR,16aS,Z)-6-(tert-butoxycarbonylamino)-14a-(cyclopropylsulfonylcarbonyl)-5,16-dioxo-1,2,3,5,6,7,8,9,10,11,13a,14,14a,15,16,16a-hexadecahydrocyclopropa[e]pyrrolo[1,2-a][1,4]diazacyclopentadecine-2-yl 4-fluoroisindoline-2-carboxylate (49). ¹H NMR (500 MHz, acetone-*d*₆) δ 10.70 (br s, 1H), 8.34 (d, 1H), 7.39–7.33 (m, 1H), 7.20 (d, 1H), 7.10–7.02 (m, 2H), 6.13 (d, 1H), 5.70 (q, 1H), 5.44 (br s, 1H), 4.99 (t, 1H), 4.78–4.59 (m, 5H),

4.18–4.08 (m, 1H), 3.88–3.81 (m, 1H), 2.86–2.78 (m, 3H), 2.71–2.60 (m, 1H), 2.52–2.35 (m, 3H), 1.92–1.81 (m, 2H), 1.75 (t, 1H), 1.61–1.14 (m, 17H), 1.04–0.95 (m, 2H). ¹³C NMR (DMSO-*d*₆, 100 MHz) δ 174.0, 172.3, 170.8, 157.5 (d, *J* = 244 Hz), 155.8, 154.0, 140.9 (d, *J* = 64.8 Hz), 130.6, 130.2, 129.6, 123.8 (d, *J* = 55.7 Hz), 119.6, 114.4 (d, *J* = 18.3 Hz), 78.4, 74.7, 59.7, 53.4, 52.7, 52.4, 49.4 (d, *J* = 37.1 Hz), 44.6, 34.9, 31.8, 30.4, 28.8, 28.6, 27.0, 25.7, 22.6, 4.8. APCI MS *m/z* 730.4 (M – 1).

■ ASSOCIATED CONTENT

Supporting Information

Biological assays, determination of aqueous solubility and pK_a values, danoprevir affinity to multiple liver uptake transporters, rodent liver PK, additional syntheses and analytical information for the tabulated inhibitors. This material is available free of charge via the Internet at <http://pubs.acs.org>.

■ AUTHOR INFORMATION

Corresponding Author

*Phone: 1-303-386-1556. E-mail: yjiang@arraybiopharma.com.

Notes

The authors declare no competing financial interest.

[§]Deceased.

■ ACKNOWLEDGMENTS

We thank all the past and present NS3/4A research team members from Array BioPharma, Inc., and InterMune, Inc., for their valuable contributions to the program.

■ ABBREVIATIONS USED

Ac, acetyl; ACN, acetonitrile; ADME, absorption, distribution, metabolism, and excretion; aq, aqueous; AUC, area under curve; BOC, *tert*-butoxycarbonyl; CDI, carbodiimidazole; CL, clearance; C_{max}, maximal concentration; CYP, cytochrome P-450; d, day; DAAs, direct acting antivirals; DBU, 1,8-diazobicyclo[5.4.0]undec-7-ene; DCE, dichloroethane; DCM, dichloromethane; DIEA, diisopropylethylamine; ER%, extraction ratio %; HATU, (O-(7-azabenzotriazol-1-yl)-N,N,N',N'-tetramethyluronium hexafluorophosphate); DMF, N,N-dimethylformamide; DMPK, drug metabolism and pharmacokinetics; DMSO, dimethylsulfoxide; EC₅₀, half-maximal effective concentration; ELISA, enzyme-linked immunosorbent assay; ER%, extraction ratio %; ESI, electrospray ionization; Et, ethyl; %F, oral bioavailability; equiv, equivalent; FDA, Food and Drug Administration; FRET, Förster resonance energy transfer; mp, melting point; HCV, hepatitis C virus; hERG, human ether-a-go-go related gene; HFBA, heptafluorobutyric acid; HPLC, high performance liquid chromatography; IC₅₀, half-maximal inhibitory concentration; h, hour; IFN, interferon; IPA, isopropyl alcohol; LCMS, liquid chromatography–mass spectrometry; PEG, polyethylene glycol; PEG IFN-α, pegylated interferon α; Ph, phenyl; PK, pharmacokinetics; RBV, ribavirin; RCM, ring-closure metathesis; rt, room temperature; SAR, structure–activity relationship; SoC, standard of care; SVR, sustained virologic response; THF, tetrahydrofuran; THIQ, tetrahydroisquinoline; TLC, thin-layer chromatography; V_{ss}, steady-state volume of distribution

■ REFERENCES

- (1) (a) *Hepatitis C Fact Sheet No. 164*; World Health Organization: Geneva, July 2012. (b) Shepard, C. W.; Finelli, L.; Alter, M. J. Global epidemiology of hepatitis C virus infection. *Lancet Infect. Dis.* **2005**, 5,

558–567. (c) Gravitz, L. A. Smoldering Public-health Crisis. *Nature* **2011**, *474*, S2–S4.

(2) (a) Fried, M. W.; Shiffman, M. L.; Reddy, K. R.; Smith, C.; Marinos, G.; Goncales, F. L.; Haussinger, D.; Diago, M.; Carosi, G.; Dhumeaux, D.; Craxi, A.; Lin, A.; Hoffman, J.; Yu, J. Peginterferon alfa-2a plus ribavirin for chronic hepatitis C virus infection. *N. Engl. J. Med.* **2002**, *347*, 975–982. (b) Manns, M. P.; McHutchison, J. G.; Gordon, S. C.; Rustgi, V. K.; Shiffman, M.; Reindollar, R.; Goodman, Z. D.; Koury, K.; Ling, M.; Albrecht, J. K. Peginterferon alfa-2b plus ribavirin compared with interferon alfa-2b plus ribavirin for initial treatment of chronic hepatitis C: a randomized trial. *Lancet*. **2001**, *358*, 958–965.

(3) (a) Welsch, C.; Jesudian, A.; Zeuzem, S.; Jacobson, I. New Direct-Acting Antiviral Agents for the Treatment of Hepatitis C Virus Infection and Perspectives. *Gut* **2012**, *61*, i36–i46. (b) Fusco, D. N.; Chung, R. T. Novel Therapies for Hepatitis C: Insights from the Structure of the Virus. *Annu. Rev. Med.* **2012**, *63*, 373–387. (c) Soriano, V.; Vispo, E.; Labarga, P.; Martin-Carbonero, L.; Fernandez-Montero, J. V.; Barreiro, P. Directly acting antivirals against hepatitis C virus. *J. Antimicrob. Chemother.* **2011**, *66*, 1673–1686. (d) Lemon, S. M.; McKeating, J. A.; Pietschmann, T.; Frick, D. N.; Glenn, J. S.; Tellinghuisen, T. L.; Symons, J.; Furman, P. A. Development of Novel Therapies for Hepatitis C. *Antiviral Res.* **2010**, *86*, 79–92.

(4) (a) Reviriego, C. Daclatasvir Dihydrochloride: Treatment of Hepatitis C Virus HCV NS5A Inhibitor. *Drugs Future* **2011**, *36*, 735–739. (b) Sofia, M. J.; Chang, W.; Furman, P. A.; Mosley, R. T.; Ross, B. S. Nucleoside, Nucleotide, and Non-Nucleoside Inhibitors of Hepatitis C Virus NS5B RNA-Dependent RNA polymerase. *J. Med. Chem.* **2012**, *55*, 2481–2531.

(5) (a) Hinrichsen, H.; Benhamou, Y.; Wedemeyer, H.; Reiser, M.; Sentjens, R. E.; Calleja, J. L.; Forns, X.; Erhardt, A.; Cronlein, J.; Chaves, R. L.; Yong, C. L.; Nehmiz, G.; Steinmann, G. G. Short-term antiviral efficacy of BILN-2061, a hepatitis C virus serine protease inhibitor, in hepatitis C genotype 1 patients. *Gastroenterology* **2004**, *127*, 1347–1355. (b) Llina-Brunet, M.; Bailey, M. D.; Bolger, G.; Brochu, C.; Faucher, A.-M.; Ferland, J. M.; Garneau, M.; Ghiro, E.; Gorys, V.; Grand-Maitre, C.; Halmos, T.; Lapeyre-Paquette, N.; Liard, F.; Poirier, M.; Rheume, M.; Tsantrizos, Y. S.; Lamarre, D. Structure–activity study on a novel series of macrocyclic inhibitors of the hepatitis C virus NS3 protease leading to the discovery of BILN 2061. *J. Med. Chem.* **2004**, *47*, 1605–1608. (c) Raboisson, P.; de Kock, H.; Rosenquist, A.; Nilsson, M.; Salvador-Oden, L.; Lin, T.-I.; Roue, N.; Ivanov, V.; Wähling, H.; Wickström, K.; Hamelink, E.; Edlund, M.; Vrang, L.; Vendeville, S.; Van de Vreken, W.; McGowan, D.; Tahri, A.; Hu, L.; Boutton, C.; Lenz, O.; Delouvroy, F.; Pille, G.; Surleraux, D.; Wigerinck, P.; Samuelsson, B.; Simmen, K. Structure–activity relationship study on a novel series of cyclopentane-containing macrocyclic inhibitors of the hepatitis C virus NS3/4A protease leading to the discovery of TMC435350. *Bioorg. Med. Chem. Lett.* **2008**, *18*, 4853–4858. (d) White, P. W.; Llinas-Brunet, M.; Amad, M.; Bethell, R. C.; Bolger, G.; Cordingley, M. G.; Duan, J.; Garneau, M.; Lagacé, L.; Thibeault, D.; Kukolj, G. Preclinical characterization of BI 201335, a C-terminal carboxylic acid inhibitor of the hepatitis C virus NS3–4A protease. *Antimicrob. Agents Chemother.* **2010**, *54*, 4611–4618. (e) Liverton, N. J.; Carroll, S. S.; DiMuzio, J.; Fandozzi, C.; Graham, D. J.; et al. MK-7009, a potent and selective inhibitor of hepatitis C virus NS3/4A protease. *Antimicrob. Agents Chemother.* **2010**, *54*, 305–311. (f) Harper, S.; McCauley, J. A.; Rudd, M. T.; Ferrara, M.; DiFilippo, M.; et al. Discovery of MK-5172, a macrocyclic hepatitis C virus NS3/4A protease inhibitor. *ACS Med. Chem. Lett.* **2012**, *3*, 332–336.

(6) (a) Gale, M.; Foy, E. M. Evasion of intracellular host defense by hepatitis C Virus. *Nature* **2005**, *436*, 939–945. (b) Thimme, R.; Lohmann, V.; Weber, F. A target on the move: innate and adaptive immune escape strategies of hepatitis C virus. *Antivir. Res.* **2006**, *69*, 129–141. (c) Li, K.; Foy, E.; Ferreon, J. C.; Nakamura, M.; et al. Immune evasion by hepatitis C virus NS3/4A protease-mediated cleavage of the toll-like receptor 3 adaptor protein TRIF. *Proc. Natl. Acad. Sci. U. S. A.* **2005**, *102*, 2992–2997.

(7) (a) Kwong, A. D.; Kauffman, R. S.; Hurter, P.; Mueller, P. Discovery and Development of Telaprevir: An NS3–4A Protease Inhibitor for Treating Genotype 1 Chronic Hepatitis C Virus. *Nature*

Biotechnol. **2011**, *29*, 993–1003. (b) Perni, R. B.; Almquist, S. J.; Byrn, R. A.; Chandorkar, G.; Chaturvedi, P. R.; Courtney, L. F.; Decker, C. J.; Dinehart, K.; Gates, C. A.; Harbeson, S. L.; Heiser, A.; Kalkeri, G.; Kolaczowski, E.; Lin, K.; Luong, Y.-P.; Rao, B. G.; Taylor, W. P.; Thomson, J. A.; Tung, R. D.; Wei, Y.; Kwong, A. D.; Lin, C. Preclinical profile of VX-950, a potent, selective, and orally bioavailable inhibitor of hepatitis C virus NS3–4A serine protease. *Antimicrob. Agents Chemother.* **2006**, *50*, 899–909. (c) Jacobson, I. M.; McHutchison, J. G.; Dusheiko, G.; Di Bisceglie, A. M.; Reddy, K. R.; Bzowej, N. H.; Marcellin, P.; Muir, A. J.; Ferenci, P.; Flisiak, R.; George, J.; Rizzetto, M.; Shouval, D.; Sola, R.; Terg, R. A.; Yoshida, E. M.; Adda, N.; Bengtsson, L.; Sankoh, a. J.; Kieffer, T. L.; George, S.; Kauffman, R. S.; Zeuzem, S. ADVANCE Study Team. Telaprevir for previously untreated chronic hepatitis C virus infection. *New Engl. J. Med.* **2011**, *364*, 2405–2416.

(8) (a) Venkatraman, S. Discovery of Boceprevir, A Direct-Acting NS3/4A Protease Inhibitor for Treatment of Chronic Hepatitis C Infections. *Trends Pharmacol. Sci.* **2012**, *33*, 289–294. (b) Venkatraman, S.; Bogen, S. L.; Arasappan, A.; Bennett, F.; Chen, K.; Jao, E.; Liu, Y.-T.; Lovey, R.; Hendrata, S.; Huang, Y.; Pan, W.; Parekh, T.; Pinto, P.; Popov, V.; Pike, R.; Ruan, S.; Santhanam, B.; Vibulbhan, B.; Wu, W.; Yang, W.; Kong, J.; Liang, X.; Wong, J.; Liu, R.; Butkiewicz, N.; Chase, R.; Hart, A.; Agrawal, S.; Ingravall, P.; Pichardo, J.; Kong, R.; Baroudy, B.; Malcolm, B.; Guo, Z.; Prongay, A.; Madision, Broske, L.; Cui, X.; Cheng, K.-C.; Hsieh, T. Y.; Brisson, J.-M.; Prelusky, D.; Korfmacher, W.; White, R.; Bogonowich-Knipp, S.; Pavlovsky, A.; Prudence, B.; Saksena, A. K.; Ganguly, A.; Piwinski, J.; Girijavallabhan, V.; Njoroge, F. G. Discovery of (1*R*,5*S*)-*N*-[3-amino-1-(cyclobutylmethyl)-2–3-dioxopropyl]-3-[2(*S*)-[[[(1,1-dimethylethyl)-amino]carbonyl]amio]-3,3-dimethyl-1-oxobutyl]-6,6-dimethyl-3-azabicyclo[3.1.0]hexan-2(*S*)-carboxamide (SCH 503034), a selective, potent, orally bioavailable, hepatitis C virus NS3 protease inhibitor: a potential therapeutic agent for the treatment of hepatitis C infection. *J. Med. Chem.* **2006**, *49*, 6074–6086. (c) Poordad, F.; McCone, J.; Bacon, B. R.; Bruno, S.; Manns, M. P.; Sulkowski, M. S.; Jacobson, I. M.; Reddy, K. R.; Goodman, Z. D.; Boparai, N.; DiNubile, M. J.; Sniukiene, V.; Brass, C. A.; Albrecht, J. K.; Bronowicki, J. P. SPRINT-2 Investigators. Boceprevir for Untreated Chronic HCV Genotype 1 Infection. *New Engl. J. Med.* **2011**, *364*, 1195–1206.

(9) (a) Seiwert, S. D.; Andrews, S. W.; Jiang, Y.; Serebryany, V.; Tan, H.; Kossen, K.; Rajagopalan, P. T. R.; Misialek, S.; Stevens, S. K.; Stoycheva, A.; Hong, J.; Lim, S. R.; Qin, X.; Rieger, R.; Condroski, K. R.; Zhang, H.; Geck Do, M.; Lemieux, C.; Hingorani, G. P.; Hartley, D. P.; Josey, J. A.; Pan, L.; Beigelman, L.; Blatt, L. M. Preclinical Characteristics of the Hepatitis C Virus NS3/4A Protease Inhibitor ITMN-191 (R7227). *Antimicrob. Agents Chemother.* **2008**, *52*, 4432–4441. (b) Rajagopalan, P. T. R.; Misialek, S.; Blatt, L. M.; Seiwert, S. D.; Kossen, K. Characterization of HCV NA3/4a protease inhibition by ITMN 191 reveals picomolar potency and slow dissociation: implications for the use of ITMN 191 in chronic HCV treatment. *Gastroenterology* **2007**, *132* (4, Supplement 1), A-782. (c) Forester, N.; Larrey, D.; Guyader, D.; Marcellin, P.; Rouzier, R.; Patat, A.; Bradford, B.; Porter, S.; Blatt, L. M.; Zeuzem, S. Treatment of Chronic Hepatitis C Virus (HCV) Genotype 1 Patients with the NS3/4A Protease Inhibitor ITMN-191 Leads to Rapid Reductions in Plasma HCV RNA: Results of a Phase 1b Multiple Ascending Dose (MAD) Study. *Hepatology* **2008**, *48*, 1132A. (d) Gane, E.; Rouzier, R.; Stedman, C.; Wiercinska-Drapalo, A.; Horban, A.; Chang, L.; Zhang, Y.; Sampeur, P.; Najera, I.; Shulman, N.; et al. Ritonavir boosting of low dose RG7227/ITMN-191, HCV NS3/4A protease inhibitor, results in robust reduction in HCV RNA at lower exposures than provided by unboosted regimens. *J. Hepatol.* **2010**, *52*, S16–S17. (e) Gane, E. J.; Roberts, S. K.; Stedman, C. A.; Angus, P. W.; Ritchie, B.; Elston, R.; Ipe, D.; Morcos, P. N.; Baher, L.; Najera, I.; Chu, T.; Lopatin, U.; Berrey, M. M.; Bradford, W.; Laughlin, M.; Shulman, N. S.; Smith, P. F. Oral combination therapy with a nucleoside polymerase inhibitor (RG7128) and danoprevir for chronic hepatitis C genotype 1 infection (INFORM-1): a randomized, double-blind, placebo-controlled, dose-escalation trial. *Lancet* **2010**, *376* (9751), 1467–1475. (f) Rajagopalan, R.; Misialek, S.; Stevens, S. K.; Myszk, D. G.; Brandhuber, B. J.; Ballard, J. A.; Andrews, S. W.; Seiwert, S. D.;

Kossen, K. Inhibition and Binding Kinetics of the Hepatitis C Virus NS3 Protease Inhibitor ITMN-191 Reveals Tight Binding and Slow Dissociative Behavior. *Biochemistry* **2009**, *48*, 2559–2568.

(10) Rubino, C.; Bradford, W.; Forrest, A.; Porter, S.; Blatt, L.; Seiwert, S.; Zeuzem, S. Pharmacokinetic-pharmacodynamic (PK-PD) relationships for ITMN-191 in a phase I multiple ascending dose trial in patients with genotype 1 chronic hepatitis C (CHC) infection. *Hepatology* **2008**, *48*, 1140A.

(11) This macrocyclization depeptidizing method has been well-known in literature and successfully applied in numerous occasions as reported in: (a) Li, P.; Roller, P. P. Cyclization strategies in peptide derived drug design. *Curr. Top. Med. Chem.* **2002**, *2*, 325–341. (b) Li, P.; Roller, P. P.; Xu, J. Current synthetic approaches to peptide and peptidomimetic cyclization. *Curr. Org. Chem.* **2002**, *6*, 411–440. (c) Grieco, P.; Cai, M.; Liu, L.; Mayorov, A.; Chandler, K.; Trivedi, D.; Lin, G.; Campiglia, P.; Novellino, E.; Hruby, V. J. Design and microwave-assisted synthesis of novel macrocyclic peptides active at melanocortin receptors: discovery of potent and selective hMC5R receptor antagonists. *J. Med. Chem.* **2008**, *51*, 2701–2707. (d) Marsault, E.; Hoveyda, H. R.; Peterson, M. L.; Saint-Louis, C.; Landry, A.; Vézina, M.; Ouellet, L.; Wang, Z.; Ramaseshan, M.; Beaubien, S.; Benakli, K.; Beauchemin, S.; Déziel, R.; Peeters, T.; Fraser, G. L. Discovery of a new class of macrocyclic antagonists to the human motilin receptor. *J. Med. Chem.* **2006**, *49*, 7190–7197. (e) Tsantrizos, Y. S.; Bolger, G.; Bonneau, P.; Cameron, D. R.; Goudreau, N.; Kukulj, G.; LaPlante, S. R.; Llinas-Brunet, M.; Nar, H.; Lamarre, D. Macrocyclic Inhibitors of the NS3 Protease as Potential Therapeutic Agents of Hepatitis C Virus Infection. *Angew. Chem., Int. Ed.* **2003**, *42*, 1355.

(12) For a systematic review to explain the rationale behind the use of bioisosteric displacement, see: (a) Patani, G. A.; LaVoie, E. J. Bioisosterism: a rational approach in drug design. *Chem. Rev.* **1996**, *96*, 3147–3176. Other recent HCV NS3-targeted DAAs utilizing the acylsulfonamide P1/P1' headgroup motif include: asunaprevir (BMS-650032) (b) McPhee, F. Identification and preclinical profile of the novel HCV NS3 protease inhibitor BMS-650032. *J. Hepatol.* **2010**, *52*, S296 and MK-5172.

(13) (a) Rieger, R. A.; Lee, P. A.; Seiwert, S. D.; Andrews, S. W.; Pope, T. K.; Pheneger, J.; Neitzel, N. N.; Franklin, R. B.; Josey, J. A.; Blatt, L. M. Pharmacokinetic analysis and liver concentrations of a series of macrocyclic peptidomimetic inhibitors of HCV NS3/4A protease: identification of ITMN-191, a potent NS3/4A protease inhibitor with high liver exposure across multiple species. *Gastroenterology* **2006**, *130* (4, Supplement 2), A-835. (b) Condroski, K. R.; Zhang, H.; Seiwert, S. D.; Ballard, J. A.; Bernat, B. A.; Brandhuber, B.; Colwell, H.; Smith, D.; Vigers, G.; Andrews, S. W.; Kennedy, A. L.; Jiang, Y.; Wenglowksy, S. M.; Josey, J. A.; Blatt, L. M. Structure-based design of novel isoindoline inhibitors of HCV NS3/4A protease and binding mode analysis of ITMN 191 by X-ray crystallography. *Gastroenterology* **2006**, *130* (4, Supplement 2), A-835.

(14) (a) Docking studies were performed using the GOLD program (version 2.0) from the Cambridge Crystallographic Data Center as described in “Development and Validation of a Genetic Algorithm for Flexible Docking” Jones, G.; Willett, P.; Glen, R. C.; Leach, A. R.; Taylor, R. *J. Mol. Biol.* **1997**, *267*, 727–748. (b) Consensus scoring performed using CScore from Tripos corporation. Five scoring functions used included FlexX Rarey, M.; Kramer, B.; Lengauer, T.; Klebe, G. *J. Mol. Biol.* **1996**, *261*, 470. (c) G_score based upon GOLD scoring (ref 14); D_score, based upon DOCK scoring Meng, C.; Shoichet, B. K.; Kuntz, I. D. *J. Comput. Chem.* **1992**, *13*, 505. (d) PMF_score Muegge; Martin, Y. C. *J. Med. Chem.* **1999**, *42*, 791. (e) ChemScore Eldridge, M. D.; Murray, C. W.; Auton, T. R.; Paolinine, G. V.; Mee, R. P. *J. Comput.-Aided Mol. Des.* **1997**, *11*, 425.

(15) Lin, C.; Gates, C. A.; Rao, B. G.; Brennan, D. L.; Fulghum, J. R.; Luong, Y.-P.; Frantz, J. D.; Lin, K.; Ma, S.; Wei, Y.-Y.; Perni, R. B.; Kwong, A. D. In vitro studies of cross-resistance mutations against two hepatitis C virus serine protease inhibitors, VX-950 and BILN 2061. *J. Biol. Chem.* **2005**, *280*, 36784–36791.

(16) Syntheses analogous to the methods described in: Faucher, A.-M.; Bailey, M. D.; Beaulieu, P. L.; Brochu, C.; Duceppe, J.-S.; Ferland, J.-M.;

Ghiro, E.; Gorys, V.; Halmos, T.; Kawai, S. H.; Poirier, M.; Simoneau, B.; Tsantrizos, Y. S.; Llinas-Brunet, M. Synthesis of BILN 2061, an HCV NS3 Protease Inhibitor with Proven Antiviral Effect in Humans. *Org. Lett.* **2004**, *6*, 2901–2904.

(17) In Figure 2, the enzymatic potency against HCV protease genotype 1b for **49** ($IC_{50} \sim 0.2$ nM) was lower than that presented in Table 4 ($IC_{50} = 1.0$ nM) as a result of its being tested in an outsourced assay with lower limit of sensitivity than our routine screening assay. For detailed assay descriptions see ref 9a.

(18) In an outsourced transportocyte assay using transfected rat and human oocytes (BD Biosciences), danoprevir demonstrated affinities to multiple liver active uptake transporters for organic anions in a concentration-dependent manner. These results are in good agreement with our in-house experiments that measure the temperature-dependent uptake of NS3 inhibitors by fresh rat hepatocytes at 4 °C (passive diffusion) vs 37 °C (passive diffusion + active uptake). From this in-house assay, the uptake at 37 °C of inhibitor **5** was about twice as much as that of both danoprevir (**49**) and inhibitor **84**.

(19) (a) Romano, K. P.; Ali, A.; Royer, W. E.; Schiffer, C. A. Drug resistance against HCV NS3/4A inhibitors is defined by the balance of substrate recognition versus inhibitor binding. *Proc. Natl. Acad. Sci. U. S. A.* **2010**, *107* (49), 20986–20991. (b) Romano, K. P.; Ali, A.; Aydin, C.; Soumana, D.; Özen, A.; Deveau, L. M.; Silver, C.; Cao, H.; Newton, A.; Petropoulos, C. J.; Huang, W.; Schiffer, C. A. The Molecular Basis of Drug Resistance against Hepatitis C Virus NS3/4A Protease Inhibitors. *PLoS Pathogens* **2012**, *8* (7), 1–15.

(20) Lim, S. R.; Qin, X.; Susser, S.; Nicholas, J. B.; Lange, C.; Herrmann, E.; Hong, J.; Arfsten, A.; Hooi, L.; Bradford, W.; Nájera, I.; Smith, P.; Zeuzem, S.; Kossen, K.; Sarrazin, C.; Seiwert, S. D. Virologic Escape during Danoprevir (ITMN-191/RG7227) Monotherapy Is Hepatitis C Virus Subtype Dependent and Associated with R155K Substitution. *Antimicrob. Agents Chemother.* **2012**, *56* (1), 271–279.

(21) In-house data. Authors from ref 19b reported danoprevir's potency shift from 1.0 to 44.8 nM (NS3/4A enzyme binding K_i) and from 0.24 to 5.7 nM (replicon IC_{50}) against WT vs A156T HCV strains.